

FINAL TECHNICAL REPORT

MIDDLE TO LATE HOLOCENE EARTHQUAKE CHRONOLOGIES FOR THE CASCADIA SUBDUCTION ZONE FROM TWO ESTUARIES IN SOUTHERN OREGON: COLLABORATIVE RESEARCH WITH WILLIAM LETTIS & ASSOCIATES, INC., AND HUMBOLDT STATE UNIVERSITY

Principal Investigators:

Robert C. Witter¹ and Harvey M. Kelsey²

¹William Lettis & Associates, Inc.,
1777 Botelho Drive, Suite 262, Walnut Creek, CA 94596;
(925) 256-6070; (925) 256-6076 fax;
witter@lettis.com

²Department of Geology
Humboldt State University, Arcata, CA 95521
(707) 826-3991
hmk1@axe.humboldt.edu

Program Elements I and II

Keywords: Fault Segmentation, Recurrence Interval, Age Dating, Regional Seismic Hazards

U.S. Geological Survey
National Earthquake Hazards Reduction Program
Award Number 02HQGR0056 (Kelsey)
Award Number 02HQGR0057 (Witter)

August 2004

Research supported by the U.S. Geological Survey, Department of the Interior, under award numbers 02HQGR0056 and 02HQGR0057. The views and conclusions contained in this document are those of the authors and should not be interpreted as necessarily representing the official policies, either expressed or implied, of the U.S. Government.

Award Numbers 02HQGR0056 and 02HQGR0057

**MIDDLE TO LATE HOLOCENE EARTHQUAKE CHRONOLOGIES FOR THE CASCADIA
SUBDUCTION ZONE FROM TWO ESTUARIES IN SOUTHERN OREGON:
COLLABORATIVE RESEARCH WITH WILLIAM LETTIS & ASSOCIATES, INC.,
AND HUMBOLDT STATE UNIVERSITY**

Robert C. Witter¹ and Harvey M. Kelsey²

¹William Lettis & Associates, Inc.,
1777 Botelho Drive, Suite 262,
Walnut Creek, CA 94596;
(925) 256-6070; (925) 256-6076 fax
witter@lettis.com

²Department of Geology
Humboldt State University
Arcata, CA 95521
(707) 826-3991
hmk1@axe.humboldt.edu

ABSTRACT

Comparisons of regional Cascadia earthquake records to earthquake chronologies at the Coquille estuary and Sixes River in southern Oregon suggest that, in contrast to the M 9 A.D. 1700 earthquake, some events ruptured shorter segments of the subduction zone and failed to trigger offshore turbidites. Between 2,000 and 4,700 years ago, earthquakes occurred on average every 350 to 415 years at the Sixes River. Over a similar time period at the Coquille estuary, earthquakes occurred on average every 525 to 650 years. When compared to the average recurrence interval of tsunamis and strong shaking reported for Bradley Lake (240 to 280 years), these distinctly different return periods at sites within 30 km of one another suggest that some earthquakes ruptured adjacent segments of the subduction zone. Corroborative evidence for segmented rupture includes age ranges, at two standard deviations, for coseismically subsided soils at the Sixes River that fail to overlap age ranges for soils at the Coquille estuary. Regional comparisons suggest that the penultimate earthquake recorded in southwestern Washington did not rupture south of Coos Bay, Oregon. Five earthquakes that occurred between 3,700 and 4,700 years ago are alternately recorded at the Sixes River and the Coquille estuary and each earthquake correlates in time with evidence for a tsunami or strong shaking at Bradley Lake. The alternating pattern of this earthquake sequence suggests a scenario where rupture termination of adjacent segments coincided at an inferred segment boundary at Cape Blanco. The Cape Blanco anticline, a transverse structural high that separates the Coquille estuary from the Sixes River, is inferred to be a possible segment boundary because it coincides with the boundary between two forearc basins that may reflect separate long-term asperities. We attribute faster relative sea-level rise at the Coquille estuary, accelerated by 0.5 to 1.3 mm/yr compared to the Sixes River, to differential uplift accommodated by one or both upper-plate structures that separate the sites, the Coquille fault and the Cape Blanco anticline. This Holocene uplift rate agrees with long-term uplift rates derived from marine terrace studies. Variations in relative sea-level curves indicate that at least two plate-boundary earthquakes triggered slip on a blind upper-plate fault that underlies the Cape Blanco anticline. Differential uplift of 0.4 to 1.7 m resulted from an earthquake 3,560 to 3,390 cal yr BP. Another earthquake produced 1.9 to 3.9 m of differential uplift about 2,470 to 2,150 cal yr BP.

TABLE OF CONTENTS

ABSTRACT.....	i
1.0 INTRODUCTION	1
2.0 CASCADIA EARTHQUAKE RECORDS	2
2.1 Coastal Marsh Records in Southwestern Oregon.....	2
2.2 Tsunami Record in a Coastal Lake	3
2.3 The Offshore Turbidite Record.....	3
2.4 Evidence for Segmented Rupture of the Cascadia Subduction Zone.....	4
3.0 RESEARCH APPROACH	5
4.0 RESULTS	7
4.1 Stratigraphic Evidence for Buried Marshes in Southwestern Oregon	7
4.1.1 Coquille River Estuary.....	7
4.1.2 Lower Sixes River Valley.....	7
4.2 Radiocarbon Age Estimates	8
4.3 Relative Sea-level Curves	9
5.0 DISCUSSION.....	11
5.1 Earthquake Recurrence Intervals: Evidence for Temporal Clustering?.....	11
5.2 Comparisons of Cascadia Earthquake Records.....	12
5.3 Coincidence of Rupture Segments and Structural Basins at Cascadia.....	14
5.4 Late Holocene Upper-plate Deformation on the Coquille Fault and the Cape Blanco Anticline	14
6.0 CONCLUSIONS.....	16
7.0 NON-TECHNICAL SUMMARY	18
8.0 ACKNOWLEDGMENTS.....	19
9.0 REFERENCES CITED.....	20

LIST OF TABLES

Table 1.	Event age estimates derived from radiocarbon data for detrital macrofossils, Coquille River estuary
Table 2.	Event age estimates derived from radiocarbon data for detrital macrofossils, Sixes River estuary

LIST OF FIGURES

Figure 1.	A: Map of the Juan de Fuca-North America Plate boundary from Vancouver Island to northwestern California, showing regional tectonic setting of the study area.
-----------	--

- B: Sevenmile Creek transect and Fahys Creek core site located along the Coquille River estuary where upper-plate structures, including the Coquille fault deform late Pleistocene marine terraces.
- C: Sixes River transect located in abandoned meander near Cape Blanco.
- Figure 2. Stratigraphy from the Coquille River estuary at Sevenmile Creek (A) and the lower Sixes River Valley near Cape Blanco (B).
- Figure 3. Detailed lithostratigraphy of vibracores collected at the Coquille River estuary and the lower Sixes River Valley.
- A: Core O from Fahys Creek and cores I and M from Sevenmile Creek together preserve stratigraphic evidence of 12 episodes of sudden marsh submergence in the last 6,300 years.
- B: Cores J, V and MM from the abandoned meander in the lower Sixes River Valley record the sudden submergence of 11 marsh soils in the last 5,500 years.
- Figure 4. Core photographs and interpretive sketches of multiple fining-upward beds within sand deposits that bury tidal marsh soils.
- A: Sand deposits overlying soils 10 and 9 in core M from the Coquille estuary at Sevenmile Creek.
- B: Four fining-upward beds overlying buried soil IX in core J at the Sixes River site.
- Figure 5. Calibrated radiocarbon-age distributions (years before AD 1950) calculated with the program OxCal (Bronk Ramsey, 2001) for detrital macrofossils selected from buried marsh soils and overlying mud and sand deposits in the lower Sixes River valley and Coquille River estuary.
- Figure 6. A: Relative sea-level curves for Coquille River estuary (blue) and lower Sixes River valley (green).
B: Reconstruction of a single sea-level curve to estimate the variation in upper-plate vertical deformation between Cape Blanco and Coquille River estuary in the last 3,000 years.
C: Reconstructing the Sixes River curve to match the elevation of the Coquille curve at about 4,300 years ago requires a shift of 0.4 to 1.7m.
- Figure 7. Frequency of earthquakes and tsunamis above the Cascadia subduction zone in southwestern Oregon.
- Figure 8. Comparison of calibrated age ranges for Cascadia subduction zone earthquakes and tsunamis at the Coquille River estuary and the lower Sixes River valley, to data from Coos Bay, Oregon and southwestern Washington.

1.0 INTRODUCTION

If $M \geq 9$ earthquakes that rupture over 900 km of the plate boundary characterize the Cascadia subduction zone, then geologic evidence of coseismic deformation in coastal marshes, offshore turbidites triggered by strong shaking, and tsunami deposits in nearshore lakes and lagoons should reflect similar paleoseismic histories. Instead, Holocene records of Cascadia earthquakes documented in southwestern Washington (Atwater and Hemphill-Haley, 1997), southwestern Oregon (Kelsey et al., 2002, in press; Nelson et al., 1998; Witter et al., 2003), northwestern California (Abramson, 1998; Garrison-Laney, 1998), and submarine canyons on the continental slope (Goldfinger et al., 2003), show distinctly different stratigraphic records that may reflect diversity in earthquake magnitude, recurrence intervals and rupture of different subduction zone segments. Contrasting histories also may evidence upper-plate folding and faulting that operate independently or in concert with subduction zone earthquakes. Such differences, whether they relate to variability in the rupture behavior of plate boundary segments or the activity of upper-plate structures overlying the megathrust, imply significantly different earthquake hazards to the Cascadia region.

Different stratigraphic records of coseismic subsidence from two coastal marshes in southwestern Oregon (Figure 1) illustrate some of the disparities among Cascadia earthquake histories that span most of the Holocene epoch. By comparing these records to records from coastal marshes in southwestern Washington, records of Cascadia tsunamis in coastal lakes and lagoons, and records of offshore turbidites, we evaluate three alternative scenarios that relate to the possible seismotectonic mechanisms at work on the Cascadia margin. First, an earthquake on a shorter segment of the plate-boundary, too small ($M \leq 8$) to trigger turbidites offshore, would cause coseismic subsidence recorded in coastal marshes above the rupture zone but not at coastal sites that overlie adjacent segments to the north or south. Yet a tsunami generated by such an earthquake could deposit sand at multiple sites along the entire length of the coast. Second, crustal deformation produced by upper-plate structures triggered by subduction zone earthquakes could significantly vary the magnitude of coseismic deformation recorded in coastal marshes. Such a scenario would leave a geologic signature that might lead to erroneous estimates of the amount of coseismic subsidence caused by subduction-related deformation alone (McNeil et al., 1998). Finally, earthquakes on upper-plate structures that operate independently of the subduction zone would likely be recorded in coastal stratigraphy but not in turbidites offshore. If, during an upper-plate earthquake, a tsunami was induced by vertical displacement of the sea floor, then deposits of sand may record coastal inundation.

In this report we present new stratigraphic and radiocarbon data from marshes at the Coquille River estuary and the lower Sixes River valley in southwestern Oregon (Figures 1B and 1C) that improve earthquake histories documented previously by Witter et al. (2003) and Kelsey et al. (2002), respectively. First, we present revised earthquake chronologies for the two sites based on AMS radiocarbon analyses of delicate detrital plant macrofossils selected from the upper surfaces of buried marshes or overlying sand layers carried in by tsunamis. Next, we contrast the relative sea-level histories of the two sites that indicate variations in the rates of Holocene vertical surface deformation of the coast. We attribute this deformation to one or more upper-plate structures that separate the sites, including the Coquille fault and the Cape Blanco anticline. Finally, we compare earthquake histories established by stratigraphic investigations in a variety of depositional environments including coastal marshes, low-lying nearshore lakes and lagoons and submarine channels. Taken together, these data suggest that past Cascadia earthquakes have been limited to discrete segments of the subduction zone and imply that some earthquakes triggered coseismic slip on upper-plate faults and deformation on overlying folds.

2.0 CASCADIA EARTHQUAKE RECORDS

Drowned forests, submerged tidal marshes, liquefaction features, offshore turbidites, and widespread tsunami-lain sand sheets characterize the geological effects caused by the A.D. 1700 Cascadia earthquake (Atwater et al., 1995; Jacoby et al., 1995; Kelsey et al., 1998; Yamaguchi et al., 1997). The earthquake, probably **M** 9 based on wave propagation modeling, generated a tsunami that traveled across the Pacific Ocean damaging coastal villages in Japan (Satake et al., 1996). In addition, radiocarbon evidence for extensive coastal subsidence (Nelson et al., 1995) indicates that the most recent Cascadia earthquake ruptured at least 680 km of the subduction zone. Despite strong agreement among data that attest to the time and size of the A.D. 1700 earthquake, paleoseismic records extending to the early and middle Holocene yield conflicting earthquake histories that resist efforts to resolve the possible rupture modes of the plate boundary. Part of this uncertainty arises from analytical error in radiocarbon dating and the uncertainty in relating the age of the dated material to the time of an earthquake (Nelson et al., 1995). Yet estuaries and lakes in southern Oregon (Kelsey et al., 2002, in press; Witter et al., 2003) contain geologic evidence for some earthquakes and tsunamis that cannot be explained by repeated characteristic **M** 9 earthquakes. The alternative hypotheses hold that past Cascadia earthquakes may have involved seismogenic segments of the subduction zone, or occurred on faults in the upper plate, or both.

2.1 Coastal Marsh Records in Southwestern Oregon

Twelve buried tidal marsh soils preserved beneath three tributary valleys of the Coquille River estuary (Figure 1B) offer a ~6,600 year stratigraphic record of estuary response to subduction zone earthquakes in southern Oregon (Witter, 1999; Witter et al., 2003). The most extensive stratigraphic sequence from the Sevenmile Creek site (Figure 2A) consists of peaty marsh soils buried by sand or mud that grades upward, in turn, to an overlying buried soil. Each soil contains fossil diatoms from high marsh or upland environments. Multiple, fining upward sandy-mud beds overlying some buried soils contain diatom fragments from sand flat environments lower in the estuary suggesting rapid deposition from an oceanward source. In all cases, thick (0.5-2.0 m) packages of estuarine mud overlie the soils and contain bivalve shells and diatoms common to mud flat environments. Sharp mud-over-peat contacts record instances of sudden relative sea-level rise and corresponding estuary expansion that persisted for decades based on thick overlying tidal flat deposits. Gradual upward transitions from estuarine mud to marsh soil indicate gradual contraction of the estuary as relative sea level fell.

The evidence for abrupt and gradual fluctuations in relative sea level records the response of the Coquille estuary to coseismic subsidence during great (**M** >8) Cascadia earthquakes and gradual uplift during interseismic periods. Evidence for widespread deposition of sand sheets suggests that some of the earthquakes triggered tsunamis that inundated the lower 10 km of the estuary. Assuming a complete stratigraphic record of coseismic subsidence events at the Coquille River estuary, time intervals between prehistoric Cascadia earthquakes have varied between about 300 years to over 1,000 years. The average earthquake-recurrence interval for the Cascadia subduction zone at the latitude of the Coquille River estuary is 570 to 590 years.

Eleven Cascadia earthquakes over the last 5,500 years have left stratigraphic signatures beneath coastal marshes in the lower Sixes River valley near Cape Blanco (Figure 1C, Kelsey et al., 2002). Within a 1.8 km² abandoned meander valley, multiple buried peaty soils that formed in fresh-water wetlands record gradual and sudden oscillations in relative sea-level that occurred ten times in the last 6,000 years (Figure 2B). An additional, youngest buried soil at the mouth of the Sixes River subsided during the A.D. 1700 Cascadia earthquake (Kelsey et al., 1998). Following the criteria of Nelson et al. (1996), all soils have multiple lines of evidence implicating tectonic subsidence as the cause of soil burial. For two of the buried soils, liquefaction of sediment accompanied subsidence. The eleven wetland soils were suddenly

buried with the last 5050 to 5600 years, yielding an average recurrence of plate-boundary earthquakes of approximately 480 to 535 years.

2.2 Tsunami Record in a Coastal Lake

Bradley Lake, situated between the Coquille River estuary and the lower Sixes River valley (Figure 1B), archives evidence of local tsunamis and seismic shaking along the southern Oregon coast over the last ~7,000 years (Kelsey et al., in press). Thirteen disturbances in the lake stratigraphy record marine incursions that resuspended lake sediment, introduced marine diatoms and deposited landward-thinning sand sheets into the lake from nearshore, beach and dune environments to the west. Four disturbances in the lake stratigraphy record episodes of strong shaking unaccompanied by tsunamis. Kelsey et al. (in press) inferred that great earthquake on the Cascadia subduction zone were the only mechanisms capable of generating the local tsunamis and strong ground motions that disturbed the lake sediments. In contrast to the 480 to 590 year average earthquake recurrence interval recorded in marshes adjacent to the lake (Kelsey et al., 2002; Witter et al., 2003), local tsunamis inundated Bradley Lake every 390 years. In the last 4,600 years, Bradley Lake was inundated by sequential tsunamis clustered in time, one following the next by a few decades to 400 years, followed by periods ranging from 700 to 1,300 years devoid of tsunamis. The thickest sand deposits and most strongly disturbed strata occur at the beginning and ends of clusters. Such evidence suggests that the most recent earthquake and tsunami (A.D. 1700) may be the first of a series of clustered tsunamis yet to occur. Kelsey et al. (in press) conclude that Bradley Lake records tsunamis generated by earthquakes that ruptured most of the length of the subduction zone as well as earthquakes that ruptured shorter segments. Perhaps the most compelling evidence for segmentation of the megathrust comes from two sand sheets deposited within a few decades of one another that may record two separate tsunamis generated by rupture of two adjoining or overlapping segments of the subduction zone.

2.3 The Offshore Turbidite Record

Sediment cores from submarine canyons between Vancouver Island and northern California contain 18 turbidites of regional extent triggered by earthquakes on the Cascadia subduction zone in the last 9,800 years (Goldfinger et al., 2003). Prior investigations of submarine landslide deposits by Adams (1990) indicate that thirteen earthquakes triggered turbidites in separate channels 150-km apart since the eruption of the Mazama ash 7,700 years ago. These data imply a 600-year average recurrence interval for these events. Goldfinger et al. (2003) conclude that synchronous triggering of turbid flows in multiple channels hundreds of kilometers apart occurred 18 times in the Holocene. They infer that the triggering mechanism for the turbidites in each case was a large earthquake ($M > 8$) that ruptured at least two-thirds of the Cascadia subduction zone. Storm-wave loading, surges of river water during storms, crustal or slab earthquakes and tsunamis from distant sources can be ruled out as alternative turbidite triggering mechanisms (Goldfinger et al., 2003). Strong circumstantial evidence supports these contentions. First, the remarkably consistent and repeating pattern of 18 Holocene turbidites from sediment cores in separate submarine channels offshore Washington and Oregon suggest repeated rupture of greater than 600 km of the plate-interface. Second, synchronous turbidite deposition in separate channels that contain the same number of events above and below channel confluences indicate that a single mechanism, most likely a large earthquake, triggered the flows. Goldfinger et al. (2003) reason that, if turbidites were triggered at different times in separate channels, the number of events recorded below a channel confluence should be the sum of the events in the two channels above the confluence. Preliminary radiocarbon results from a sediment core in Juan de Fuca Canyon (JFC, Figure 1A), uncorrected for ^{14}C reservoir effects and basal erosion, show a repeating pattern in recurrence intervals that consists of clusters of 3 to 4 earthquakes closely-spaced in time. Repeat times between earthquakes in a cluster range from 200 to 500 years; longer intervals between clusters range from 800 to 1,500 years. Although these data do not preclude past rupture of segments of the subduction zone, the remarkably consistent number and apparent synchronicity

of turbidites in separate offshore channels implies little variability in rupture length for earthquakes that triggered the turbidites.

2.4 Evidence for Segmented Rupture of the Cascadia Subduction Zone

Geological evidence from coastal Oregon and historical earthquake sequences observed at subduction zones that switch rupture modes imply that, unlike the A.D. 1700 event, some past Cascadia earthquakes may have ruptured segments of the plate boundary (e.g., Nelson and Personius, 1998; Ruff, 1996; Thatcher, 1990). For example, Nelson and Personius (1998) postulated the location of a segment boundary near the latitude of the Alsea River (between 44° and 45°N) based on differences in marsh stratigraphic records documented in northern and southern coastal Oregon. Comparison between the average return time for tsunamis at Bradley Lake (380 to 400 years) and the average earthquake recurrence interval (480 to 590 years) from adjacent estuaries led Kelsey et al. (in press) to conclude that the lake strata record earthquakes that ruptured variable lengths of the Cascadia margin. These results support contentions by Kelsey et al. (2002) and Witter et al. (2003) that some plate-boundary earthquakes recorded in coastal estuaries of southern Oregon did not rupture the entire length of the subduction zone. Based on comparisons of regional Cascadia earthquake histories, Witter et al. (2003) suggested that segment boundaries at the latitude of Cape Blanco and Heceta Head may limit northward or southward directed rupture. These data leave open the possibility that rupture lengths and recurrence times during past Cascadia earthquake sequences have varied, similar to historical earthquake sequences at the Columbia-Ecuador subduction zone (Kanamori and McNally, 1982) and the Nankai Trough (Ando, 1975).

Offshore gravity lows centered on five sedimentary basins in the Cascadia forearc provide physical evidence for distinct seismogenic segments of the subduction zone (Figure 1A). Studies of great subduction zone earthquakes worldwide show a strong correlation between the location of sedimentary basins that coincide with gravity lows in the forearc and areas of high coseismic slip interpreted to be long-term asperities (Wells et al., 2003). Wells et al. (2003) recognized similarities between the organization of offshore basins and transverse structural highs along the Cascadia margin and forearc structures along the Nankai Trough (Sugiyama, 1994) that correlate with areas of high moment release during historical earthquakes. In Cascadia, the largest asperity is 300 km long and is located offshore Washington and northern Oregon (gravity low C, Figure 1A). This potential rupture patch is bound by transverse structural highs at Quinault on the north and Heceta Head on the south. Another candidate rupture segment exists offshore south-central Oregon between structural highs at Heceta Head on the north and Cape Blanco on the south (gravity low D, Figure 1A). Wells et al. (2003) propose that the Cascadia margin may be separated structurally into three major segments that extend from Vancouver Island to Heceta Head, Heceta Head to Cape Blanco, and Cape Blanco to Cape Mendocino (gravity lows C, D, and E₁₋₃, respectively, Figure 1A). The evidence for structural segmentation of the subduction zone, indicated by large offshore gravity lows, is consistent with geological evidence for rupture mode diversity (Nelson and Personius, 1998; Kelsey et al., 2002, in press; Witter et al., 2003) and implies that future earthquakes may involve both single- and multiple-segment ruptures.

3.0 RESEARCH APPROACH

Our approach tests the hypothesis that the Cascadia subduction zone always generates M 9 earthquakes that rupture most of the length (>600 km) of the plate boundary. If the hypothesis is true, then marsh stratigraphic records of sudden coseismic subsidence should reflect identical earthquake chronologies at different sites along the coast from Vancouver Island to northern California. In addition, these records should correlate one-for-one with offshore turbidite sequences triggered by great earthquakes (Goldfinger et al., 2003) and a record of local earthquake-induced tsunamis preserved in Bradley Lake (Kelsey et al., in press). Testing the hypothesis is warranted because details of the Sixes River paleoseismic record (Kelsey et al., 2002) appear to be incompatible with paleoseismic records to the north at the Coquille River estuary (Witter et al., 2003) and at Willapa Bay (Atwater and Hemphill-Haley, 1997). The Coquille River estuary and the lower Sixes River valley offer a unique opportunity to test the hypothesis because they are only 30 km apart, yet at the same time appear to overlie a candidate segment boundary at Cape Blanco, and are separated from southwestern Washington by another candidate segment boundary at Heceta Head (Figure 1). To disprove the hypothesis, we must demonstrate that radiocarbon-derived chronologies for plate-boundary earthquakes documented in southern Oregon and at Willapa Bay are not correlative within the uncertainties of ^{14}C dating (e.g., Nelson, 1992).

To demonstrate discordance in time between an earthquake recorded in southwestern Oregon and a possible correlative earthquake recorded at separate sites along the Cascadia margin, we compared calibrated radiocarbon age ranges for earthquakes recorded at multiple sites, and evaluated how closely these ages reflect the actual time of coseismic subsidence. To most accurately estimate earthquake ages, we used identifiable detrital plant macrofossils, too delicate to be recycled, sampled from within 0.02 m above or below the upper contact of a buried soil. The results of previous investigations that dated detrital macrofossils (Kelsey et al., 2002; Kelsey et al., in press; Witter et al., 2003) suggest the most reliable material includes herbaceous seeds, conifer or deciduous tree leaves, and small woody twigs with bark and stem nodes intact. We assume this material falls to the ground near the site at the time, or just before (years), the soil was submerged and buried. Seed and conifer needle species were identified (Dunwiddie, 1985; Faber, 1996; Hickman and Jepson, 1993; Pojar and MacKinnon, 1994) to ensure that the detritus came from a plant that likely grew locally in the wetland just prior to coseismic subsidence. If the age ranges do not overlap at two standard deviation uncertainty, then the soils with disparate ages cannot record the same earthquake. If, over a given time interval, the numbers of earthquakes recorded at separate sites differ, and the stratigraphic record of earthquakes at each site appears to be complete, then some earthquakes may have ruptured some individual segments of the plate boundary and not others.

Alternatively, coastal stratigraphic records of earthquakes may reflect local vertical land-level changes accommodated by displacement on upper-plate faults, whether triggered by earthquakes on the Cascadia megathrust or operating independently. At least two upper-plate structures, the Coquille fault and the Cape Blanco anticline, separate the Coquille River estuary from the Sixes River valley (Figures 1A and 1B). To evaluate possible variations in vertical deformation of the coast accommodated by these structures, we compared relative sea-level curves constructed for the two study sites using new radiocarbon data as well as data from Kelsey et al. (2002) and Witter et al. (2003). If the Cape Blanco anticline or the Coquille fault has been active in the Holocene, then the vertical component of surface deformation may result in different relative sea-level histories at the Coquille estuary and Sixes River. Because the two sites lie within 30 km of one another, we assume that any influence on relative sea level related to glacio-isostatic processes or in response to tectonic strain accumulation and release on the underlying subduction zone should be identical at both sites. Therefore, in the absence of Holocene deformation on upper-plate structures, the two relative sea-level histories should be identical. Any discrepancies between the two relative sea-level curves would characterize the timing and magnitude of vertical deformation caused by Holocene displacement on upper-plate faults. The relative sea-level curves

presented here use sea-level index points defined by the elevations and ages of the upper contacts of buried soils to track the elevation of mean tide level through time.

4.0 RESULTS

4.1 Stratigraphic Evidence for Buried Marshes in Southwestern Oregon

Stratigraphy observed in nine vibracores from the Coquille River estuary and six vibracores from the lower Sixes River valley confirm evidence for extensive and repeated late Holocene submergence of coastal marshes in southwestern Oregon documented by Witter et al. (2003) and Kelsey et al. (2002) (Figure 2). Stratigraphic sequences beneath the Coquille River estuary and the lower Sixes River valley consist of marsh soils abruptly buried by thick packages of estuarine sand and mud that gradually grade upward into the next overlying marsh soil (Figure 3). The term “soil” refers to peat or organic mud deposited in tidal marsh or freshwater wetland environments as determined by diatom paleoecological data reported by Kelsey et al. (2002) and Witter et al. (2003). In many cases, sand layers overlying the soils that contain brackish-marine diatoms, include multiple fining-upward beds indicating deposition by successive surges of water. Each buried soil records sudden drowning of the marshes caused by rapid relative sea level rise. In contrast, the thick deposits of sand and mud that grade upward into the next marsh soil record slow aggradation of the estuary and relative sea-level fall. Individual soils were correlated on the basis of lithostratigraphic characteristics, lateral continuity, depth and age. At the Coquille estuary, drowning of extensive tidal marshes occurred twelve times in the last ~6,700 years. Similarly, at the Sixes River, twelve episodes of rapid relative sea-level rise changed freshwater wetlands into tidal flats in the last ~6,200 years.

4.1.1 Coquille River Estuary

Nine vibracores from the Coquille River estuary preserve stratigraphic evidence for 12 instances of sudden marsh submergence (Figure 3A). Three sediment cores from each of three sites contain nearly identical stratigraphy to that documented by Witter et al. (2003). Exceptions include the identification of soil 9 (Figure 4A) and a discontinuous sand layer not associated with a buried soil (layer i, Figures 2A and 3A), both in core M. Soil 9 in core M consists of peaty mud and is overlain by four fining upward sequences of sand to muddy sand (Figure 4A). Previous investigations observed soil 9 in core K, N, R, and P to the north (Figure 2A) but no organic material was sampled from the soil or overlying sand deposits for radiocarbon analysis to estimate the timing of submergence. The identification of soil 9 in core M extends correlation of the soil approximately 300 m to the south. Detrital plant macrofossils were sampled from the overlying sand deposit and submitted for radiocarbon dating.

Several discontinuous sand layers (layers g, i, and m, Figures 2A and 3A), recognized in previous cores (Witter et al., 2003), provide limited stratigraphic markers to help correlate soils among cores. The deposits vary in thickness from <0.1 to 0.01 m and range in texture from silty fine-grained sand to sandy silt. In some cases the deposits have sharp lower contacts. All of these discontinuous sand layers interrupt thick deposits of mud that overlie and bury marsh soils with one exception: sand layer i in core M occurs in the lower part of soil 7 (Figure 3A). The sand layers do not occur in each core and, where sand layers were observed, the layers were absent in some cores when repeated cores were collected at the same site. Of 15 cores at the Sevenmile Creek site (Figure 2A), layer g occurred in three, layer i occurred in five, layer m occurred in two and layer o occurred in one. Despite the discontinuous nature of the sand deposits, four out of five layers can be correlated between cores that are ~800 to ~1,300 m apart.

4.1.2 Lower Sixes River Valley

Six vibracores from the lower Sixes River valley provide stratigraphic evidence for 11 instances of sudden relative sea-level rise that submerged freshwater marshes (Figure 3B). Two sediment cores each from sites J, V and MM (Figure 4B) contain marsh soils buried by intertidal mud and sand that

corroborate soil correlations documented by Kelsey et al. (2002). Slight differences between cores collected during this investigation and cores studied by Kelsey et al. (2002) demonstrate the discontinuous nature of some soils and overlying sand deposits across distances of 1,100 to 1,200 m.

Several buried soils and overlying sand deposits evident in the cores (that were not observed by previous workers) strengthen previous soil correlations (Kelsey et al., 2002). In core J, a sand deposit consisting of four fining-upward beds overlies soil IX (Figure 4B). The irregular lower contact between sand and soil and peat rip-up clasts within the sand indicate erosion during deposition. Also in core J, an anomalous sandy mud layer, about 0.1-m thick, that contained a 25-mm long rounded pebble did not overlie a buried soil. However, the stratigraphic position of the sand layer suggests that it correlates with sand layers overlying soil XI documented in cores to the northeast (Figure 2B). Finally, the vibracores at site J documented by this study did not contain soil VIIa identified in prior cores taken at the site by Kelsey et al. (2002). We interpret that soil VIIa is of very limited extent and does not represent widespread submergence of the wetland.

New observations of buried soils and sand deposits in cores V and MM also strengthen correlations among cores. A new vibracore at site V reaches a depth of 4.40 m, over one meter deeper than prior cores, and contains buried soil XI and an overlying sand deposit that included two fining-upward beds (Figure 3B). A 0.01-m thick sand layer overlying soil VIII was observed in core MM that had not been observed previously. Finally, two distinct buried soils and overlying sand deposits in the lower 1.4 m of core MM correlate with soils IX and X in adjacent cores and improve soil correlations over those reported previously (Kelsey et al., 2002).

4.2 Radiocarbon Age Estimates

AMS radiocarbon analyses of 32 detrital plant macrofossils supplement radiocarbon data published by Kelsey et al. (2002) and Witter et al. (2003). The integrated data set (Tables 1 and 2) includes a total of 85 C^{14} ages and provides a basis to reevaluate age estimates using calibration and statistical tools in the program OxCal v. 3.9 (Bronk Ramsey, 2001). The new results include age estimates for soil 9 at the Coquille River estuary and soils II and IV at the Sixes River site—soils that have not been dated prior to this investigation. Of the new data, all but four of the fourteen dates from Coquille River cores and all but seven of the eighteen dates from the Sixes River cores are in stratigraphic order indicating that most of the material in the dated samples provide maximum limiting age estimates that likely predate the time of soil burial by less than several hundred years.

We used OxCal (Bronk Ramsey, 2001) with the INTCAL98 radiocarbon calibration data set of Stuiver et al. (1998) to evaluate the stratigraphic consistency of all ages and to restrict the calibrated age ranges that estimate the time of soil burial (Figure 5). For the OxCal analysis we organized the integrated Coquille estuary data set (Table 1) into twelve groups (soils 1 through 12 plus sand layer i) in stratigraphic order, with the ages in each group unordered. Similarly, we organized the integrated Sixes River data set (Table 2) into eleven groups representing soils II through XII. We calculated the means of statistically similar ages likely from the same population that were indistinguishable at the 95% level based on a chi-squared test (Ward and Wilson, 1978). Calibrated radiocarbon ages were determined for the means and for younger and older ages within the same group that were statistically different from the mean ages. Ages considered out of stratigraphic order showed low (<16%) probabilities of being in the correct sequence and were not used in the final OxCal analysis. Reworking by either tidal processes or erosion and redeposition by inferred tsunamis best explains the older samples in this category (e.g., the two oldest ages for soil 9, Table 1). Samples that showed evidence of bomb radiocarbon (modern) also were eliminated. All other ages in the integrated data sets showed probabilities of >98% of being in the correct stratigraphic order. The far right column in both Tables 1 and 2 lists the preferred calibrated age ranges for buried soils at both study sites.

Three ages interpreted to be anomalously young, yet stratigraphically consistent based on OxCal sequence analyses, were identified in both data sets and require additional explanation. In two cases, the youngest age for Coquille soil 3 and the youngest age for Sixes soil X (Tables 1 and 2, respectively), the ages were significantly younger than mean ages of multiple older samples that were indistinguishable at 95% level based on chi-squared tests. Both samples consisted of herbaceous seeds that, we interpret, were contaminated with younger organic material introduced during the initial collection and/or processing of the materials. Another anomalously young age came from hemlock needles of soil 4 from a core along Ferry Creek investigated by Witter et al. (2003). We chose to use the age on twigs from soil 4 in core I based on more robust stratigraphic correlations documented in Sevenmile Creek cores and because there is no direct stratigraphic correlation between soils at Sevenmile Creek and soils at Ferry Creek about 7 km to the south.

Average sedimentation rates are used to estimate the age range for the time of burial of soil II at the Sixes River site (Figure 5). The age is based on the mean depth ranges of upper soil contacts and calibrated age distributions for soils VII to III. Prior to 3,500 yr BP sedimentation occurred at an average rate of 1.2 mm/yr. After 3,500 yr BP sediment accumulated more slowly at about 0.6 mm/yr. Comparisons show that, for both periods before and after 3,500 yr BP, calibrated radiocarbon age estimates agree well with age estimates derived from average sedimentation rates (Figure 5).

4.3 Relative Sea-level Curves

Relative sea-level curves constructed for both sites show repeated instances of sudden relative sea-level rise followed by periods of gradual relative sea-level fall (Figure 6). Marsh stratigraphic sequences reflect these changes in relative sea level based on different fossil diatom assemblages in the buried soils versus the overlying mud and sand (Figures 3A and 3B). The sharp contact between soil and overlying deposits indicates sudden relative sea-level rise. Quantitative counts of fossil diatoms show that most of the soils formed in low to high tidal marsh or freshwater wetland environments (Kelsey et al. 2002; Witter et al., 2003). Overlying deposits of sand and mud from the tidal flat indicate rapid submergence of the soil. Gradual relative sea-level fall is indicated by the gradual upward transition from intertidal mud to overlying high marsh or freshwater peat (Kelsey et al. 2002; Witter et al., 2003).

The upper contacts of the buried soils define the relative sea-level curve at each site because the contacts are paleo-sea-level index points (Figure 6). Two sea-level index points can be determined for each contact between soil and overlying sand or mud. Assemblages of high tidal marsh and freshwater diatoms in the soil directly below the contact indicate the elevation of sea level prior to marsh submergence; assemblages of tidal flat diatoms in the overlying mud directly above the contact indicate the elevation of sea level after submergence.

The relative sea-level curves (Figure 6A) consist of a series of rectangles that represent the estimated age and depth of the upper contacts of buried soils (sea-level index points) relative to modern mean tide level (MTL). The height and width of rectangles represent the magnitude of the error in the position of paleo-MTL in time versus elevation space. The width of a rectangle equals the calibrated age estimate for soil submergence (Tables 1 and 2). The height of a rectangle estimates the relative elevation of MTL based on fossil diatom assemblages from soils (before submergence) and overlying deposits of mud (after submergence) reported previously (Kelsey et al., 2002; Witter et al., 2003). Broad, overlapping elevation ranges for the intertidal zones correspond to fossil diatom assemblages and encompass the uncertainty in the relative elevation of MTL (Witter et al., 2003). Both relative sea-level curves show long-term trends of relative sea-level rise through the middle Holocene, punctuated by instances of rapid relative sea-level rise followed by short-term relative sea-level fall. In the last 3,000 to 3,500 years, the rate of relative sea-level rise has decreased at the Coquille estuary. In contrast, over the same period of time the Sixes River curve indicates a reversal in trend evident as relative sea-level fall.

The two relative sea-level curves show different rates and trends of relative sea-level change at two sites, approximately 30 km apart, separated by active upper-plate structures (Figure 6). Comparison of the Sixes and Coquille curves (Figure 6B) shows that, for ages older than ~3,000 cal yr BP, sea-level index points at Sixes are 2 to 4 m higher than those of equivalent age at Coquille. Further comparison of the superposed curves (Figure 6C) shows that, for ages older than ~4,300 cal yr BP, sea-level index points of equivalent age are 0.4 to 1.7 m higher at the Sixes River than at the Coquille estuary. In addition, a significant decrease in the rate of relative sea-level rise at the Sixes River occurs between 4,300 and 3,800 cal yr BP, followed by an increase in the rate of rise between 3,800 and 3,000. No variation in the rate of relative sea-level rise occurred over the same time period at the Coquille site.

One explanation for the differences in the two relative sea-level curves is variation in the rates of vertical deformation of the coast accommodated by combined displacement on upper-plate folds and faults and on the subduction zone megathrust. Barring vertical tectonic surface deformation, the two curves should be identical because responses to post-glacial isostatic adjustment and regional deformation related to the seismic cycle of the subduction zone should affect both sites equally. Differences between the two curves indicate two instances of vertical surface deformation that influenced relative sea level at the Sixes site relative to the Coquille site. At least one instance occurred in the last ~3,000 years based on a 2- to-4-m upward vertical shift in the Sixes curve relative to the Coquille curve (Figure 6B). Another instance occurred between 4,300 and 3,800 years ago based on a 0.4- to-1.7-m upward vertical shift of the Sixes curve after reconstructing a single curve for both sites (Figure 6C). In both instances, restoring the Sixes curve to match the Coquille curve requires downward shifts that indicate at least two episodes of up-to-the-south vertical surface deformation with magnitudes of 3 ± 1 m and 1 ± 0.6 m.

5.0 DISCUSSION

The results of this investigation support the conclusions of Kelsey et al. (2002) and Witter et al. (2003) that multiple earthquakes in southwestern Oregon dropped tidal marshes, low-lying forests and freshwater wetlands into the lower intertidal zone. Our results strengthen the case for twelve Cascadia subduction zone earthquakes at the Coquille River estuary in the last 6,730 to 6,490 cal yr BP and twelve earthquakes at the Sixes River in the last 6,180 to 5,930 cal yr BP—the youngest event at the Sixes site is evident as a soil buried by tsunami sand near the river mouth (Kelsey et al., 1998). At both sites, the youngest buried soil records coseismic subsidence and tsunami inundation caused by the A.D. 1700 Cascadia earthquake (Nelson et al., 1995; Kelsey et al., 1998). In all cases, evidence for coseismic subsidence includes changes in fossil diatom assemblages across sharp (<3 mm) upper contacts of buried soils that indicate submergence by rapid relative sea-level rise. The submergence lasted decades to hundreds of years based on fossil diatoms and bivalves that persist in thick (0.1 to 0.5 m) deposits of intertidal mud overlying the soils. Evidence for submergence of entire estuaries and sites separated by tens of kilometers suggests the effects were widespread. The maximum magnitude of subsidence at both sites ranged from 2.3 to 3 m based on reconstructions of relative sea level using biostratigraphic and radiocarbon data. Such long lasting, widespread and large amounts of submergence rule out climatic processes that influence sea level, including El Niño, and storms or local fluctuations in the tidal range related to changes in barrier spits (Nelson et al., 1996), as explanations for soil submergence. Layers of sand abruptly overlying most soils that possess characteristics of tsunami deposits indicate that earthquakes dislocated the seafloor. Finally, comparison of soil ages to regional Cascadia earthquake records suggests that some of the buried soils record rupture of hundreds of kilometers of the plate boundary.

5.1 Earthquake Recurrence Intervals: Evidence for Temporal Clustering?

Continuous and detailed stratigraphic records at the Coquille estuary and the Sixes River reflect complete earthquake histories that represent reliable earthquake recurrence intervals. Stratigraphic sequences at both sites are not interrupted by unconformities that would indicate erosion or periods of no deposition. However, an earthquake that occurred within 150 years of a prior earthquake may not be represented in the record because tidal marshes may not have been set to record coseismic subsidence (Atwater et al., 2001; Witter et al., 2003). Earthquake sequences with longer recurrence intervals likely provided sufficient time to reestablish marsh conditions that would record coseismic subsidence.

The average earthquake recurrence interval for the Coquille estuary is 570 to 590 years (Witter et al. (2003). We calculate the mean recurrence interval by subtracting the age of the A.D. 1700 earthquake (250 yr BP) from the maximum and minimum age estimates for the oldest earthquake (6,730 to 6,490 cal yr BP), then dividing each result by the number of earthquakes in the record prior to the most recent event (11). The longest return time may have exceeded 1,200 years (e.g., maximum difference between ages for soils 4 and 5 and soils 10 and 11; Table 1). In contrast the age of soil 9 overlaps the age of soil 10 suggesting that a few decades may have separated some earthquakes. Considering post-earthquake rates of sedimentation in drowned estuaries, brackish marshes in southern Oregon probably require 50 to 150 years to reach conditions conducive to recording coseismic subsidence (Atwater et al., 2001; Witter et al., 2003). This observation suggests that 50 to 150 years represent the practical lower limit for repeat times of earthquakes recorded by marsh soils.

The mean recurrence interval of plate boundary earthquakes at the Sixes River is 515 to 540 years for twelve earthquakes using the 6,180 to 5,930 cal yr BP age range for the oldest earthquake. Similar to the Coquille earthquake record, the longest interval between earthquakes at the Sixes River exceeded 1,200 years (e.g., the maximum difference between the age of the penultimate earthquake, 1,520 to 1,000 cal yr

BP, and the A.D. 1700 earthquake). The minimum difference between the ages of soils VIII and VII and soils V and IV provide the shortest recurrence intervals that are less than 70 years.

Local tsunamis inundated Bradley Lake on average every 380 to 400 years over the last 4,630 to 4,460 years (Kelsey et al., in press), much more frequently than the average recurrence of earthquakes inferred from coseismic subsidence at the Coquille estuary ~10 km to the north or the Sixes River ~20 km to the south. Similar to the earthquake histories reconstructed at neighboring estuaries (Kelsey et al., 2002; Witter et al., 2003) and elsewhere along the Cascadia subduction zone (Atwater and Hemphill-Haley, 1997; Nelson et al., 1998), individual tsunami recurrence intervals ranged from a few decades to 1200 years. Between 4,600 and 2,800 cal yr BP at Bradley Lake, tsunamis came in clusters of 3 to 4 every 1,000 years (Figure 7) (Kelsey et al., in press). Sets of closely spaced tsunamis were followed by longer periods that spanned 670 to 1,260 years with no tsunamis. Some of these gaps in the tsunami record at Bradley Lake overlap gaps in the Coquille earthquake record, for example between 2,960 and 2,310 and 6,190 and 5,300. The time coincidence of gaps in both records suggests that some earthquake sequences north of Bradley Lake involved variable recurrence patterns of several earthquakes grouped in time. In contrast, earthquakes at the Sixes River appear to fill the periods when tsunamis did not enter Bradley Lake and the Coquille estuary experienced seismic quiescence (Figure 7). Sixes River earthquakes that appear to be out of phase with the tsunami record suggests that some earthquakes had magnitudes that were too small to trigger tsunamis high enough to incur Bradley Lake. Recurrence patterns in the earthquake history at the Coquille estuary suggest that earthquakes north of Bradley Lake may be clustered in time. The Sixes earthquake record by comparison shows a recurrence pattern that is more equally distributed through time.

Thirteen turbidites triggered by subduction zone earthquakes in the last 7,700 years have an average recurrence interval of ~600 years (Adams, 1990; Goldfinger et al., 2003). Although the turbidite record represents the longest paleoseismic record for the Cascadia subduction zone, the record probably is not a complete one of all plate-boundary earthquakes. The earthquake records from southwestern Oregon have significantly shorter average repeat times over similar lengths of record. Because the turbidite sequences record fewer earthquakes than records of coseismic subsidence and tsunamis from estuaries and coastal lakes, we infer that some events were likely below the threshold magnitude for triggering submarine landslides.

Earthquake recurrence intervals at the Sixes River differ from those at the Coquille estuary and Bradley Lake between ~2,000 and ~4,700 years ago (Figure 7). Eight earthquakes at the Sixes River occurred on average every 350 to 415 years over this time period. In contrast, only five earthquakes occurred at Coquille during that time period with much longer average recurrence intervals between 525 and 650 years. For comparison, evidence for tsunamis and strong shaking at Bradley Lake between 2,800 to 4,600 years ago show repeat times between 240 to 280 years—much shorter than either the Coquille or the Sixes earthquake records. The disparities in these recurrence intervals suggest that the Sixes chronology records earthquakes on a southern segment of the subduction zone that did not rupture northward beyond the latitude of the Coquille estuary and Bradley Lake may record the sum of events documented at the Sixes River and at the Coquille estuary. Therefore, Cascadia earthquakes that rupture variable lengths of the subduction zone may be the best explanation for different recurrence intervals evident in southwestern Oregon (Kelsey et al., 2002, in press; Witter et al., 2003).

5.2 Comparisons of Cascadia Earthquake Records

Geologic records from other Pacific Northwest estuaries, nearshore lakes and lagoons and turbidite sequences in submarine channels provide comparative Holocene earthquake histories for the Cascadia subduction zone. Investigations of subsidence stratigraphy at Willapa Bay, Copalis River, Grays Harbor and the Columbia River (Figure 1A) document evidence for eight earthquakes in the last ~4,000 years in

southwestern Washington (Atwater and Hemphill-Haley, 1997; Atwater, 2003, personal commun.). The ages of two older subsided peat horizons extend the Washington record to ten earthquakes in the last ~5,000 years ago (Shennan et al., 1996). Tidal marsh stratigraphy at Coos Bay, Oregon records nine earthquakes in the last ~4,800 years, including some that likely record subsidence above upper-plate folds (Nelson et al., 1996, 1998; A. Nelson, 2003, personal commun.). Lagoon Creek in northwestern California (Figure 1A) records six Cascadia tsunamis over the last ~3,400 years (Abramson, 1998; Garrison-Laney, 1998). We compare these records to the 6,200- and 6,700-year earthquake histories documented at the Sixes River and the Coquille estuary, respectively, to evaluate the variability in rupture lengths of past Cascadia earthquakes (Figure 8). We do not include the Juan de Fuca Canyon turbidite record (Figure 1A) of 18 subduction zone earthquakes in the last 9,800 years (Goldfinger et al., 2003) because the published ages of turbidites have not been corrected for carbon reservoir effects or basal erosion.

Overlapping radiocarbon-derived age estimates (at two standard deviations) from different records imply that several earthquakes ruptured more than 610 km of the subduction zone (Figure 8). For instance, the A.D. 1700 earthquake (**M** 9) ruptured most of the length (probably 800 to 900 km) of the Cascadia subduction zone (Nelson et al., 1995; Satake et al., 1996). Overlap among ages for earthquakes about 1,300 to 1,200 and 3,500 to 3,400 years ago also suggest long-length rupture of the Cascadia margin (Figure 8), possibly during **M** 9 earthquakes. Yet disparities in number of earthquakes and non-overlapping age ranges make it difficult to correlate other earthquakes over distances greater than 400 km of the subduction zone.

Some age estimates show little or no overlap with other age ranges (at two standard deviations) among widely separated sites and may reflect past rupture of separate seismogenic segments of the Cascadia margin. The clearest examples include earthquake III at Sixes, earthquakes 4 and IV at Coquille and Sixes, respectively, and earthquake IX at Sixes. It is possible that nearly identical ages on a twig and possibly reworked wood fragments in Sixes soil III (Table 2) predate the age of coseismic subsidence by a few hundred years. However, even if this possibility were true, we tentatively correlate Sixes III with a tsunami deposit recorded at Bradley Lake (Kelsey et al., in press) that lacks a definitive correlative earthquake at sites to the north. Clear overlap between ages for Sixes IV, Coquille 4, and part of Coos Bay 5 allow the possibility that one earthquake ruptured at least 60 km of the megathrust in south-central Oregon. But, with the exception of the broad age range for Coos Bay 5, these ages do not overlap ages in southwestern Washington and instead appear to fill a noticeable gap in the earthquake record. Sixes earthquake IX does not overlap ages of earthquakes recorded in southwestern Washington or the Coquille estuary. Such mismatched age estimates for earthquakes in southern Oregon lead us to the conclusion that some earthquakes did not rupture the entire length of the subduction zone.

The strongest case for rupture of separate segments of the subduction zone along the southern Oregon coast involves the apparent alternating sequence of five earthquakes that occurred between ~3,700 and ~4,700 years ago. Comparisons of the Coquille estuary, Bradley Lake and Sixes River records show that evidence for coseismic subsidence appears to alternate in time between the Sixes and Coquille and that each earthquake produced a tsunami or, in one case, shaking strong enough to disturb sediments in Bradley Lake (Figure 7). The alternating pattern and serial progression of inferred earthquake rupture patches in the 3,700 to 4,700 year-age interval (Figure 7) depict rupture of segments of the subduction zone separated by a segment boundary located between the Coquille estuary and the Sixes River.

Does the Cascadia subduction zone always rupture most of its length during **M** 9 earthquakes? Such behavior would contrast with historical earthquake sequences documented at subduction zones worldwide, including the Nankai Trough (Ando, 1975), and the Columbia-Ecuador plate boundary (Kanamori and McNally, 1982), that include earthquakes with variable rupture lengths that cluster in time. Turbidites in offshore marine canyons may record 18 great earthquakes in the last 9,800 years, each

possibly **M** 9, that ruptured most of the length of the margin (Goldfinger et al., 2003). At this time, maximum limiting radiocarbon ages for turbidites, not corrected for carbon reservoir effects or basal erosion, preclude meaningful comparisons with onshore records to better constrain the timing of the largest Cascadia earthquakes. However, we postulate that several “extra” earthquakes in southern Oregon left no record in offshore channels because they ruptured discrete segments that produced shaking intensities too low and durations too short to trigger turbidites.

5.3 Coincidence of Rupture Segments and Structural Basins at Cascadia

Gravity anomalies that coincide with forearc basins define at least five structural segments of the Cascadia subduction zone (Wells et al., 2003). Empirical data from subduction zone earthquakes with high moment release worldwide show spatial correlations between forearc basins identified by low gravity and seismogenic asperities. Three segments offshore southern Washington, Oregon and northern California are indicated by gravity lows C, D and E₁₋₃ (Figure 1A). The boundaries between these three segments are inferred to coincide with transverse structural highs at Heceta Head, and Cape Blanco (Figure 1A) (Wells et al., 2003). Comparisons of earthquake histories (discussed above; Figures 7 and 8) show that some earthquakes recorded at the Sixes River (Figure 1C) are absent in stratigraphic records at the Coquille estuary (Figure 1B) and suggest that the two sites lie on either side of a segment boundary near the latitude of Cape Blanco. The data imply that some past Cascadia earthquakes ruptured the segment or segments that underlie gravity lows E₁₋₃ but did not rupture segments to the north. Paleoseismic records also show that rupture during other earthquakes terminated north of Cape Blanco and did not rupture segments to the south.

Several inferred earthquake sequences are consistent with rupture terminations at boundaries of gravity-defined structural basins. For instance, earthquakes that subsided soils III, IX and X at the Sixes River may record rupture of a segment or segments underlying gravity lows E₁₋₃ (Figure 1A). At least one earthquake recorded at the Sixes River and Coquille estuary may have ruptured parts of segments underlying gravity lows D and E, but probably did not rupture the northern segment overlying gravity low C. As postulated by Witter et al. (2003), our data allow the interpretation that rupture during event W in southwestern Washington did not propagate south of Coos Bay because the Coquille and Sixes marshes did not subside between 1,000 and 250 cal yr BP. Yet other earthquakes, like the A.D. 1700 event, likely ruptured at least three or more Cascadia segments underlying offshore gravity lows. Weighing all paleoseismic evidence documented along the Cascadia subduction zone leads us to the conclusion that earthquakes of variable rupture length are possible and probabilistic seismic hazard assessments should include source models with a diversity of segment rupture modes.

5.4 Late Holocene Upper-plate Deformation on the Coquille Fault and the Cape Blanco Anticline

At least two Quaternary upper-plate structures, the Coquille fault and the Cape Blanco anticline, separate the two study sites. Holocene movement on these structures is evident from coastal geologic studies (Kelsey et al., 2002; Witter et al., 2003), but how much vertical deformation can be attributed to slip on the underlying faults, and do they rupture during subduction zone earthquakes or independently? The Coquille fault vertically deforms the 80,000-year-old Whiskey Run marine platform by about 50 m at the entrance to the Coquille estuary (McInelly and Kelsey, 1990) and possibly raised late Holocene fluvial sediments at Ferry Creek (Witter et al., 2003), a tributary to the Coquille River located on the south (up-thrown) side of the fault. The Cape Blanco anticline deforms late Pleistocene marine platforms and terrace sediments (Kelsey, 1990); late Holocene contraction of the anticline, probably triggered by subduction zone earthquakes, caused different amounts of marsh subsidence on the southern limb of the fold (Kelsey et al., 2002). We compare relative sea-level curves at both sites (Figure 6) to estimate the magnitude of differential vertical deformation and evaluate whether slip on upper-plate faults likely was triggered by coseismic rupture of the megathrust or occurred independently. We assume that, in the

absence of Holocene deformation on upper-plate structures, the relative sea-level curves at the two sites should be identical because regional deformation related to the accumulation and release of strain on the subduction zone and post-glacial isostatic adjustments in southern Oregon should produce similar effects at both sites separated by 30 km. Because the Sixes River site overlies the axis of the Cape Blanco anticline and because the Coquille estuary site is located on the down-thrown (north) side of the Coquille fault, any Holocene vertical deformation on these structures should reflect higher relative sea-level elevations at the Sixes site relative to the Coquille site, based on sea-level index points of similar age.

Differences between the two curves indicate that upper-plate surface deformation produced 1.9 to 3.9 m of differential uplift at the Sixes site relative to the Coquille estuary in the last ~3,000 years (Figure 6B). Between ~4,300 and 3,000 years ago, surface deformation raised the Sixes site 0.4 to 1.7 m relative to the Coquille site (Figure 6C). We attribute the differences in the relative sea-level curves to late Holocene slip on one or both upper-plate structures located between the two sites. Long-term uplift rates derived from studies of late Pleistocene marine terraces (0.3 to 1.2 mm/yr; Kelsey 1990; McNelly and Kelsey, 1990), agree well with the differential uplift rate of 0.5 to 1.3 mm/yr estimated from variations in relative sea-level change in the last 4,410 to 4,150 years (age of Sixes soil IX). This rate reflects the sum of the uplift rate of the Sixes site that overlies the axis of the Cape Blanco anticline and the rate of subsidence of the Coquille site located on the down-thrown side of the Coquille fault. Therefore, assuming the long-term uplift rate at Cape Blanco (0.5 to 1.2 mm/yr; Kelsey et al., 1990) approximates the late Holocene uplift rate, and by subtracting that rate from the rate of differential uplift between the two sites (0.5 to 1.3 mm/yr), we infer that the Coquille site subsided at a rate of <0.1 mm/yr over the last 4,300 years.

Paleoseismic data at Sixes River indicate that the Cape Blanco anticline coseismically contracted at 3,560 to 3,390 years ago and at 2,470 to 2,150 years ago (Kelsey et al., 2002) and these times of deformation coincide with the two periods when relative sea-level rise at Sixes River diverged from relative sea-level rise at Coquille estuary (Figures 6B and 6C). Was slip on upper-plate faults triggered by rupture of the megathrust or did the crustal faults rupture independently? We concur with the deformation model of Kelsey et al. (2002) whereby, a subduction zone earthquake triggers synchronous coseismic slip on a blind reverse fault in the upper plate that contracts the overlying Cape Blanco anticline. The amount of local uplift related to contraction of the anticline is less than the magnitude of regional subsidence related to strain release above the megathrust because each earthquake sequence produced net subsidence recorded by buried soils at the Sixes River. The distinct lack of geologic evidence for net coseismic uplift including Holocene fluvial or marine terraces, raised marine platforms, or emergent tidal flats abruptly lifted to elevations of high marsh environments corroborates the contention that slip on the upper-plate faults accompanied rupture of the megathrust.

6.0 CONCLUSIONS

The results of this investigation include thirty-two AMS radiocarbon ages that provide data to evaluate earthquake recurrence patterns, compare regional earthquake histories, and evaluate segmentation models for the Cascadia subduction zone. We also use the data to contrast two relative sea-level curves that show differences in vertical surface deformation that we attribute to movement on upper-plate structures that separate the Coquille estuary and the Sixes River. This study contributes new information on the recurrence patterns and rupture modes of Cascadia earthquakes that will be used in next-generation seismic hazard maps for western North America.

Unlike the **M** 9 earthquake in A.D. 1700, comparisons of regional Cascadia earthquake records suggest that some events ruptured shorter segments of the plate-interface that failed to trigger offshore turbidites. Such events are most evident in the different histories of coseismic subsidence documented in southwestern Oregon at the Coquille estuary and the Sixes River. The differences between the records include variations in earthquake frequency through time, age estimates that do not overlap one another at two standard deviations, and evidence for a series of earthquakes, alternately recorded at the Sixes and Coquille sites that each caused disturbances in the sedimentary record of Bradley Lake. In the first case, significantly more earthquakes occurred at the Sixes River between ~2,000 and ~4,700 years ago, on average one every 350 to 415 years, than at the Coquille estuary where earthquakes occurred on average every 525 and 650 years over a similar time period. Evidence for tsunamis and strong shaking indicate much shorter repeat times (240 to 280 years) at Bradley Lake, located between the two estuaries, over that same period. These distinctly different recurrence intervals suggest that Bradley Lake records evidence for earthquakes that ruptured adjacent segments of the plate-interface: some occurred to the south and tectonically subsided the Sixes River valley while others occurred to the north and coseismically lowered marshes at the Coquille estuary. In the second case, age estimates for several buried soils at the Sixes River do not overlap age ranges for soils at the Coquille estuary. In one case where Sixes soil IV does overlap Coquille soil 4, consistent with synchronous subsidence at both sites, the ages do not overlap preferred age ranges of earthquakes in southwestern Washington. Although there is some overlap between soil ages for the penultimate events recorded at most sites, we infer that the earthquake that subsided soil W in southwestern Washington did not rupture south of Coos Bay, Oregon. Finally, between 3,700 and 4,700 years ago five earthquakes are recorded separately at the Sixes River and the Coquille estuary. Age estimates for these events with little or no overlap suggest that the five earthquakes alternated between sites, first on a segment underlying the Sixes River then on a segment underlying the Coquille estuary, and so on. Each earthquake correlates with a tsunami deposit or evidence for strong shaking recorded at Bradley Lake, located between the two sites.

The Coquille estuary and the Sixes River are separated by the Cape Blanco anticline, a structural high oriented transverse to the Cascadia margin, identified by Wells et al., (2003) to be a possible segment boundary. Offshore gravity lows that coincide with forearc basins define five possible seismogenic segments of the Cascadia plate boundary (Wells et al., 2003). At least three are present offshore southwestern Washington, Oregon and northwestern California. Because regional earthquake histories are not identical at widely separate sites, the hypothesis that the Cascadia plate boundary only produces **M** 9 earthquakes fails. Comparisons of earthquake histories in southwestern Oregon and elsewhere along the Cascadia margin show compelling evidence for past earthquakes that produced limited rupture of a segment south of Cape Blanco. Other earthquakes appear to have overlapping or adjacent segments in southern Oregon. The penultimate earthquake may have been limited to the largest segment located offshore southwestern Washington and northwestern Oregon.

At least two late Holocene earthquakes involved slip on a blind, upper-plate fault that underlies the Cape Blanco anticline, causing localized folding and uplift evident by higher paleo-sea-level elevations relative

to the Coquille estuary. One earthquake occurred between ~4,300 and 3,000 years ago; at least one other event occurred after ~3,000 years ago. The timing is consistent with two upper-plate events that occurred 3,560 to 3,390 cal yr BP and 2,470 to 2,150 cal yr BP inferred from differential subsidence of wetland soils (Kelsey et al., 2002). The earthquakes probably accompanied plate-boundary earthquakes that subsided marsh soils at the Sixes River because no evidence of coseismically uplifted terraces or emergent tidal flats exist in the lower valley. Comparisons of relative sea-level curves at the Sixes River and the Coquille estuary show differential uplift rates equal to 0.5 to 1.3 mm/yr. This range in the Holocene uplift rate agrees well with published long-term uplift rates derived from marine terrace studies. The different relative sea-level histories do not conclusively show evidence for late Holocene movement on the Coquille fault. However, the Coquille estuary, located on the northern (downthrown) side of the fault, appears to have subsided at a rate of about 0.1 mm/yr in the last 4,300 years.

7.0 NON-TECHNICAL SUMMARY

Geologic records of Cascadia subduction zone earthquakes recorded at the Coquille estuary and the Sixes River in southwestern Oregon differ from records along the coasts of southwestern Washington and northern California. The different earthquake records indicate that not all past events were as large as the most recent magnitude 9 earthquake that extended along the entire fault length (>900 km) in A.D. 1700. Instead, comparisons reveal variations in earthquake frequency and mismatches in timing that suggest that the plate-boundary may be subdivided into sections, or fault segments, that are capable of generating large earthquakes that impact a few hundreds of kilometers of coastline rather than the entire length of the fault. For example, an earthquake recorded in southwestern Washington and central coastal Oregon about 1,000 years ago is not recorded at coastal sites in southern Oregon suggesting that the earthquake was limited to a segment in the northern part of the plate boundary. Between 4,700 and 3,700 years ago, records show that a sequence of five earthquakes alternated between the Sixes River and Coquille estuary and each earthquake can be linked to evidence for a tsunami or strong shaking recorded in a coastal lake located between the sites. The alternating pattern of the earthquake sequence suggests that a boundary between fault segments may separate the Coquille estuary and the Sixes River. Geophysical data suggest that this boundary coincides with the Cape Blanco anticline because this structure separates two offshore basins interpreted to reflect plate-boundary segments that have experienced repeated earthquakes. The elevation of sea level relative to land has risen over the past several thousand years, but sea level rose 0.5 to 1.3 mm/yr faster at the Coquille estuary than at the Sixes River. We attribute the disparity in rates of sea level change to deformation on the Cape Blanco anticline and the Coquille fault, two structures that separate the study sites and overlie the subduction zone. Based on differences in the rates of sea level change at the two sites, we interpret that at least two plate-boundary earthquakes triggered movement on a buried fault that underlies the Cape Blanco anticline about 3,500 years ago and 2,300 years ago. The earthquake that occurred 3,500 years ago caused 1.9 to 3.9 m of uplift at the Sixes River relative to the Coquille estuary; the event 2,300 years ago produced 0.4 to 1.7 m of uplift.

8.0 ACKNOWLEDGMENTS

Grants to Kelsey and Witter from the U.S. Geological Survey (NEHRP 02HAGR0056 and NEHRP 02HAGR0057) supported this research. The views and conclusions contained in this document are those of the authors and should not be interpreted as necessarily representing the official policies, either expressed or implied, of the U.S. Government. Cape Blanco State Park allowed access to park property at the Sixes River. J. Daugherty allowed access to property along Sevenmile Creek. E. Kelsey, C. Pritchard, and M. Larsen assisted in the field and laboratory.

9.0 REFERENCES CITED

- Adams, J., 1990, Paleoseismicity of the Cascadia subduction zone: Evidence from turbidites off the Oregon-Washington margin: *Tectonics*, 9, p. 569-583.
- Atwater, B. F., and Hemphill-Haley, E., 1997, Recurrence intervals for great earthquakes of the past 3500 years at northeastern Willapa Bay, Washington: United States Geological Survey Professional Paper 1576, 108 p.
- Atwater, B. F., Stuiver, M., and Yamaguchi, D. K., 1991, Radiocarbon test of earthquake magnitude at the Cascadia subduction zone: *Nature*, 353, p. 156-158.
- Atwater, B.F., and 15 others, 1995, Summary of coastal geologic evidence for past great earthquakes at the Cascadia subduction zone: *Earthquake Spectra*, 11, p. 1-18.
- Atwater, B.F., Yamaguchi, D.K., Bondevik, S., Barnhardt, W.A., Amidon, L.J., Benson, B.E., Skjerdal, G., Shulene, J.A., and Nanayama, F., 2001, Rapid resetting of an estuarine recorder of the 1964 Alaska earthquake: *Geological Society of America Bulletin*, v. 113, p. 1193-1204.
- Blakely, R.J., Christiansen, R.L., Guffanti, M., Wells, R.E., Donnelly-Nolan, J.M., Muffler, L.J.P., Clyne, M.A., and Smith, J.G., 1997, Gravity anomalies, Quaternary vents, and Quaternary faults in the southern Cascade range, Oregon and California: Implications for arc and backarc evolution: *Journal of Geophysical Research*, 102, p. 22,513-22,527.
- Bronk Ramsey, C., 2001, Development of the radiocarbon calibration program OxCal: *Radiocarbon*, 43, p. 355-363.
- Dunwiddie, P.W., 1985, Dichotomous key to conifer foliage in the Pacific Northwest: *Northwest Science*, 59, p. 185-191.
- Faber, P.M., 1996, *Common Wetland Plants of Coastal California*, Second Edition, Pickleweed Press, Mill Valley, California, 122 pp.
- Goldfinger, C., Nelson, C.H., Johnson, J.E. and the Shipboard Scientific Party, 2003, Holocene earthquake records from the Cascadia subduction zone and northern San Andreas fault based on precise dating of offshore turbidites, *Annu. Rev. Earth Planet. Sci.* v. 31, p. 555-577.
- Hickman, J.C. and W.L. Jepson (eds), 1993, *The Jepson Manual: Higher Plants of California*, University of California Press, 1400 pp.
- Jacoby, G., Carver, G., and Wagner, W., 1995, Trees and herbs killed by an earthquake ~300 yr ago at Humboldt Bay, California: *Geology*, 23, p. 77-80.
- Kelsey, H.M., 1990, Late Quaternary deformation of marine terraces on the Cascadia subduction zone near Cape Blanco, Oregon: *Tectonics*, 9, p. 983-1014.
- Kelsey, H.M., Witter, R.C., and Hemphill-Haley, E., 1998, Response of a small Oregon estuary to coseismic subsidence and post seismic uplift in the last 300 years: *Geology*, 26, p. 231-234.
- Kelsey, H.M., Sherrod, B., Johnson, S.Y., and Dadisman, S.V., 2004, Land-level changes from a late Holocene earthquake in the northern Puget Lowland, Washington: *Geology*, v. 32, n. 6, p. 469-472.
- Kelsey, H.M., Nelson, A.R., Hemphill-Haley, E. and Witter, R.C., in press, Tsunami history of an Oregon coastal lake reveals a 4,600 year record of great earthquakes on the Cascadia subduction zone: *Geological Society of America Bulletin*.

- Kelsey, H.M., R.C. Witter, and E. Hemphill-Haley, 2002, Plate-boundary earthquakes and tsunamis of the past 5500 yr, Sixes River estuary, southern Oregon: *Geological Society of America Bulletin*, 114, 3, p. 298-314.
- McInelly, G.W. and Kelsey, H.M., 1990. Late Quaternary tectonic deformation in the Cape Arago-Bandon region of coastal Oregon as deduced from wave-cut platforms: *Journal of Geophysical Research*, 95, p. 6699-6713.
- McNeil, L.C., Goldfinger, C., Yeats, R.S., and Kulm, L.D., 1998, The effects of upper-plate deformation on records of prehistoric Cascadia subduction zone earthquakes, *in* Stewart, I., and Vita-Finzi, C., eds., *Coastal Tectonics: Geological Society of London Special Publication*, v. 146, p. 321-342.
- Miller, M.M., Johnson, D.J., Rubin, C.M., Dragert, H., Wang, K., Qamar, A., and Goldfinger, C., 2001, GPS-determination of along-strike variation in Cascadia margin kinematics: Implications for relative plate motion, subduction zone coupling, and permanent deformation: *Tectonics*, v. 20, p. 161-176.
- Nelson, A. R., 1992, Discordant ^{14}C ages from buried tidal-marsh soils in the Cascadia subduction zone, southern Oregon coast: *Quaternary Research*, v. 38, p. 74-90.
- Nelson, A.R., Shennan, I. and Long, A.J., 1996, Identifying coseismic subsidence in tidal-wetland stratigraphic sequences at the Cascadia subduction zone of western North America: *Journal of Geophysical Research*, 101, p. 6115-6135.
- Nelson and 11 others, 1995, Radiocarbon evidence for extensive plate-boundary rupture about 300 years ago at the Cascadia subduction zone: *Nature*, 378, p. 371-374.
- Pojar, J., and A. MacKinnon (eds), 1994, *Plants of the Pacific Northwest Coast*, British Columbia Ministry of Forests, Lone Pine Publishing, Edmonton, Alberta, 527 pp.
- Ruff, L.J., 1996, Large earthquakes in subduction zones: Segment interaction and recurrence times, *in* G.E. Bebout et al. (eds), *Subduction: Top to Bottom*, Geophysical Monograph 96: American Geophysical Union, p. 91-104.
- Satake K., Shimazaki, K., Tsuji, Y., and Ueda, K., 1996, Time and size of a giant earthquake in Cascadia inferred from Japanese tsunami records of January 1700: *Nature*, 379, p. 246-251.
- Shennan, I., Long, A. J., Rutherford, M. M., Green, F. M., Innes, J. B., Lloyd, J. M., Zong, Y., and Walker, K. J., 1996, Tidal marsh stratigraphy, sea-level change and large earthquakes, I: a 5000 year record in Washington, USA: *Quaternary Science Reviews*, v. 15, p. 1023-1059.
- Stuiver, M., and Reimer, P.J., 1993. Extended ^{14}C data base and revised Calib 3.0 ^{14}C age calibration program: *Radiocarbon*, 35, p. 215-230.
- Stuiver, M., Reimer, P.J., Bard, E., Beck, J.W., Burr, G.S., Hughen, K.A., Kromer, B., McCormac, F.G., v. d. Plicht, J., and Spurk, M., 1998. INTCAL98 Radiocarbon age calibration 24,000 - 0 cal BP: *Radiocarbon*, 40, p. 1041-1083.
- Sugiyama, Y., 1994, Neotectonics of Southwest Japan due to the right-oblique subduction of the Philippine Sea plate: *Geofisica Internacional*, 33, p. 53-76.
- Wells, R.E., Blakely, R.J., Sugiyama, Y., Scholl, D.W. and Dinterman, P.A., Basin-centered asperities in great subduction zone earthquakes: A link between slip, subsidence, and subduction erosion?: *Journal of Geophysical Research*, v. 108, n. B10, ESE 16, p. 1-30.
- Wells, R.E., Weaver, C.S., and Blakely, R.J., 1998, Fore-arc migration in Cascadia and its neotectonic significance: *Geology*, 26, p. 759-762.

- Witter, R. C., 1999, Late Holocene paleoseismicity, tsunamis and relative sea-level changes along the south-central Cascadia subduction zone, southern Oregon, U.S.A.: Ph.D. dissertation, Eugene, University of Oregon, 178 p.
- Witter, R.C., H.M. Kelsey, and E. Hemphill-Haley, 2003, Great Cascadia earthquakes and tsunamis of the past 6,700 years, Coquille River estuary, southern coastal Oregon: *Geological Society of America Bulletin*, 115, 10, p. 1289-1306.
- Yamaguchi, D.K., Atwater, B.F., Bunker, D.E., Benson, B.E., and Reid, M.S., 1997, Tree-ring dating the 1700 Cascadia earthquake: *Nature*, 389, p. 922-923.

TABLES

Table 1. Event age estimates derived from radiocarbon data for detrital macrofossils, Coquille River estuary

Buried soil no.*	Radiocarbon lab number [#]	Core Number [†]	Sample depth in core (m)	Material dated	$\delta^{13}\text{C}$ (‰)	Lab-reported age (^{14}C yr BP at 1σ) [§]	Calibrated age (cal yr BP at 2σ) ^{**}	OxCal age (cal yr BP at 2σ) ^{###}
2	GX30699	FC-03-OC	0.735	unid. rhizome	-27.6	modern	Not used	
	GX31030	FC-03-OB	0.74-0.75	herbaceous seeds	-27.4	1190 ± 30 ^{††}	1230-990	1340-1000
	<i>GX 24244</i>	<i>FC-98-O</i>	0.79-0.83	<i>spruce needles</i>	-28.8	<i>1340 ± 50</i>	1350-1170	
3	GX30700	FC-03-OC	1.01	unid. Rhizome	-24.7	modern	Not used	
	<i>GX23843</i>	<i>SM-97-M</i>	0.77-0.80	<i>seeds</i>	-30	<i>1540 ± 50</i>	1530-1310	
	GX31028	SM-03-IC	0.76-0.77	herbaceous seeds, spruce needles	-24	1690 ± 40 ^{††}	1710-1520	1700-1530
	<i>GX23844</i>	<i>FC-97-G</i>	0.75-0.78	<i>seeds</i>	-29.2	<i>1700 ± 50</i> ^{††}	1740-1510	
	<i>GX 24245</i>	<i>FC-98-O</i>	1.12-1.14	<i>spruce needles</i>	-27.9	<i>1710 ± 50</i> ^{††}	1740-1510	
4	<i>GX24171</i>	<i>BA-97-S</i>	0.97-1.05	<i>hemlock needles</i>	-28.1	<i>1940 ± 40</i>	Not used	
	GX31022	SM-03-IB	1.28	twigs	-24.1	2150 ± 40 ^{††}	2310-2000	2310-2000
	<i>GX23845</i>	<i>FC-97-G</i>	1.26-1.29	<i>seeds</i>	-27.5	<i>2290 ± 50</i>	2370-2150	
	GX31021	SM-03-IB	1.26	twig	-28.2	2530 ± 40	2750-2460	
	GX31029	SM-03-IC	1.175-1.185	delicate detrital charcoal	-25.4	2580 ± 40	2780-2490	
5	<i>GX23846</i>	<i>FC-97-K</i>	2.13-2.19	<i>seeds, conifer needle</i>	-26.4	2840 ± 50 ^{††}	3140-2790	3210-2960
	<i>GX23792</i>	<i>SM-97-A</i>	1.87-1.90	<i>pine needles, seeds</i>	-28.4	2890 ± 40 ^{††}	3210-2880	
	<i>GX24172</i>	<i>BA-97-S</i>	1.83-1.86	<i>spruce needles</i>	-28.8	2970 ± 50 ^{††}	3330-2960	
	<i>GX24238</i>	<i>BA-97-H</i>	-0.03	<i>spruce needles</i>	-28.5	3010 ± 50 ^{††}	3360-3030	
6	<i>GX22596</i>	<i>BA-96-G</i>	2.22-2.24	<i>moss</i>	-30.1	3200 ± 50 ^{††}	3560-3270	3560-3390
	<i>GX23793</i>	<i>SM-97-M</i>	1.44-1.46	<i>seeds, pine and cedar leaves</i>	-28.1	3230 ± 40 ^{††}	3560-3360	
	<i>GX23600</i>	<i>SM-97-I</i>	2.12-2.16	<i>conifer needles, seeds</i>	-28.6	3240 ± 50 ^{††}	3630-3350	
	<i>GX23847</i>	<i>FC-97-G</i>	2.26-2.38	<i>seeds, conifer needle</i>	-27.9	3250 ± 50 ^{††}	3630-3360	
	<i>GX24173</i>	<i>BA-97-S</i>	2.13-2.15	<i>spruce needles</i>	-27.9	3350 ± 50 ^{††}	3700-3460	
	<i>GX22594</i>	<i>BA-96-H</i>	0.75-0.80	<i>cone fragment</i>	-25.4	<i>3460 ± 50</i>	3870-3580	
7	<i>GX23794</i>	<i>SM-97-M</i>	1.98-2.00	<i>pine needles</i>	-29.6	3650 ± 50 ^{††}	4150-3830	4090-3900
	GX31025	SM-03-IA	3.035	spruce needles, seed	-25.1	3660 ± 40 ^{††}	4150-3860	
	<i>GX23601</i>	<i>SM-97-I</i>	2.98-3.00	<i>fir needles, cone fragments</i>	-25.8	3670 ± 50 ^{††}	4150-3840	
	GX31023	SM-03-IB	3.005	spruce needles, cone fragment	-28.4	3710 ± 50	4230-3890	
sand i	GX31027	SM-03-MC	2.49-2.51	herbaceous seeds	-25.9	3750 ± 40 ^{††}	4240-3890	4240-3980

Table 1. Event age estimates derived from radiocarbon data for detrital macrofossils, Coquille River estuary

Buried soil no.*	Radiocarbon lab number [#]	Core Number [†]	Sample depth in core (m)	Material dated	$\delta^{13}\text{C}$ (‰)	Lab-reported age (^{14}C yr BP at 1σ) [§]	Calibrated age (cal yr BP at 2σ) ^{**}	OxCal age (cal yr BP at 2σ) ^{###}
8	<i>GX23795</i>	<i>SM-97-M</i>	3.23-3.26	<i>moss</i>	-26.5	<i>2360 ± 50</i>	Not used	
	<i>GX23848</i>	<i>FC-97-G</i>	2.56-2.62	<i>alder and willow leaves</i>	-28.8	4000 ± 50 ^{††}	4790-4290	4610-4410
	<i>GX23532</i>	<i>SM-97-I</i>	4.17-4.19	<i>conifer needles</i>	-28.3	4060 ± 50 ^{††}	4810-4410	
	<i>GX24239</i>	<i>BA-97-H</i>	0.87-0.96	<i>seeds</i>	-28.9	4060 ± 60 ^{††}	4820-4410	
	<i>GX31024</i>	<i>SM-03-IB</i>	4.145	<i>spruce needles, cone fragment, seed</i>	-23.7	4190 ± 40	4840-4570	
9	<i>GX30698</i>	<i>SM-03-MB</i>	3.93-3.94	<i>conifer needles</i>	-29.1	4430 ± 40 ^{††}	5280-4860	5240-4860
	<i>GX31026</i>	<i>SM-03-MC</i>	3.95-3.96	<i>conifer needles</i>	-27.7	4570 ± 40	Not used	
	<i>GX30697</i>	<i>SM-03-MB</i>	3.92-3.93	<i>herbaceous seeds</i>	-29.7	4630 ± 40	Not used	
10	<i>GX23796</i>	<i>SM-97-M</i>	4.05-4.08	<i>pine and fir needles, moss</i>	-28.7	4460 ± 40 ^{††}	5300-4870	5300-5040
	<i>GX23849</i>	<i>FC-97-H</i>	3.03-3.07	<i>seeds</i>	-28	4480 ± 50 ^{††}	5310-4880	
	<i>GX23602</i>	<i>SM-97-I</i>	5.32-5.37	<i>needles, moss, cone fragment</i>	-28.1	4520 ± 50 ^{††}	5320-4980	
	<i>GX24240</i>	<i>BA-97-H</i>	2.33-2.37	<i>seeds</i>	-28.9	4520 ± 50 ^{††}	5320-4980	
	<i>GX24174</i>	<i>BA-97-S</i>	4.24-4.33	<i>seeds</i>	-30.6	5050 ± 40	5910-5660	
11	<i>GX24241</i>	<i>BA-97-S</i>	5.46-5.49	<i>hemlock and spruce needles</i>	-28.4	5390 ± 50 ^{††}	6290-5990	6310-6190
	<i>GX23533</i>	<i>SM-97-I</i>	6.72-6.74	<i>conifer needles, cone fragment</i>	-29.2	5500 ± 50 ^{††}	6410-6190	
	<i>GX22595</i>	<i>BA-96-H</i>	4.76-4.80	<i>conifer needles</i>	-28.3	5530 ± 60 ^{††}	6450-6190	
12	<i>GX23534</i>	<i>SM-97-I</i>	7.71-7.73	<i>conifer needles, seed</i>	-29.4	5770 ± 50 ^{††}	6720-6440	6730-6490
	<i>GX23797</i>	<i>SM-97-M</i>	7.14-7.18	<i>pine, fir, cedar leaves, moss</i>	-28.5	5830 ± 50 ^{††}	6750-6490	

Note: data shown in italics from Witter et al. (2003).

*Radiocarbon age data grouped by buried soil number determined by stratigraphic correlation. Soil numbers increase with age.

[#]Lab abbreviation: GX, Geochron Laboratories, Cambridge, Massachusetts.

[†]Core number designates locality, year sampled, and specific core identified by letter. The localities are abbreviated as follows: SM, Sevenmile Creek; FC, Fahys Creek; BA, Ferry Creek.

[§]Conventional ages reported by radiocarbon laboratory based on the Libby half life (5570) for ^{14}C . Bold ages are statistically indistinguishable at the 95% confidence level based on a chi-square test (Ward and Wilson, 1978).

**Calibrated age ranges before AD 1950 reported to the nearest decade, computed with OxCal (Bronk Ramsey, 2001) using the INTCAL98 radiocarbon calibration dataset of Stuiver et al. (1998) with a lab error multiplier of 1.0 and reported to 2σ .

###Preferred calibrated age ranges based on stratigraphic analysis of radiocarbon ages and the means of statistically indistinguishable ages, where available, using OxCal (Bronk Ramsey, 2001).

^{††}Lab-reported ages used in OxCal analyses.

Table 2. Event age estimates derived from radiocarbon data for detrital macrofossils, Sixes River estuary

Buried soil no.*	Radiocarbon lab number [#]	Core Number [†]	Sample depth in core (m)	Material dated	$\delta^{13}\text{C}$ (‰)	Lab-reported age (^{14}C yr BP at 1σ) [§]	Calibrated age (cal yr BP at 2σ) ^{**}	OxCal age (cal yr BP at 2σ) ^{##}
II	GX30361	02 VD	0.560	seeds	-28.6	modern	Not used	1520-1000 ^{§§}
	GX30362	02 VD	0.570	seeds	-29.5	modern	Not used	
III	GX30363	02 VD	1.08	seeds	-25.8	250 ± 30	Not used	2130-1930
	GX22923	96 GG	0.760	twig	-26.2	2065 ± 45***	2150-1900	
	AA17183	94 V	0.780	wood fragment, seed	-27.4	2070 ± 45***	2150-1920	
	GX30596	02 VB	1.205	tree stems/twigs	-26.6	2360 ± 30	2710-2330	
IV	GX30250	02 VD	1.190	seeds	-26.7	1640 ± 50	Not used	2470-2150
	GX30250	02 VD	1.190	seeds	-26.7	2310 ± 60***	2750-2100	
V	B47082	91 A	3.750	roots	-25.0*	2450 ± 80***	2740-2350	2750-2360
	GX19892	93 A	3.550	roots	-26.8	2499 ± 66***	2750-2360	
	GX24243	95 BB	1.325	seeds	-26.3	2520 ± 40***	2750-2400	
	GX30252	02-VB	1.540	seeds	-28.2	3110 ± 70	Not used	
VI	GX23048	95 BB	1.585	papery husks, seed	-28.0	2880 ± 50***	3210-2860	3170-2870
	GX22925	96 GG	1.535	~170 <i>Carex</i> spp. Seeds	-27.6	2885 ± 45***	3210-2870	
	GX30256	02 MMZ	1.485	deciduous leaves	-26.4	3080 ± 40	3390-3160	
	GX30253	02 MMZ	1.485	tree stems/twigs	-27.4	3150 ± 30	3470-3260	
VII	AA17186	94 V	1.550	spruce needles	-29.1	3175 ± 65***	3560-3240	3560-3390
	GX23049	95 BB	1.890	seeds	-26.2	3240 ± 50***	3630-3350	
	GX25682	98 MM	1.585	spruce needle fragments	-28.7	3240 ± 40***	3570-3360	
	GX24243	95 J	3.000	seeds	-29.4	3250 ± 40***	3580-3370	
	GX23045	96 J	3.010	spruce needles, seeds, leaves	-29.6	3340 ± 50***	3690-3460	
VIII	GX30364	02 VD	2.365	seeds	-26.6	modern	Not used	3880-3630
	GX19890	93 J	3.910	spruce needles, twigs, cone	-27.4	3419 ± 67***	3840-3470	
	GX20201	94 V	2.090	twigs with bark	-27.5	3546 ± 64***	3990-3630	
	GX30597	02 MMZ	2.140	tree stem/twig	-26.8	3610 ± 30	3990-3830	
IX	GX20200	93 S	2.910	herb stem	-27.6	3732 ± 89***	4450-3800	4410-4150
	GX25683	98 MM	2.245	spruce needles, cone, seeds	-26.2	3780 ± 50***	4360-3980	
	GX22946	96 JJ	2.525	spruce needles, cone, seeds	-26.8	3840 ± 50***	4420-4090	
	GX20202	94 V	2.560	spruce needles, twig, seed	-28.3	3864 ± 63***	4440-4080	
	AA19420	95 BB	2.760	twig with bark	-27.1	3875 ± 55***	4440-4090	
GX23046	95 J	4.350	seeds	-26.8	3900 ± 40***	4430-4150		

Table 2. Event age estimates derived from radiocarbon data for detrital macrofossils, Sixes River estuary

Buried soil no.*	Radiocarbon lab number [#]	Core Number [†]	Sample depth in core (m)	Material dated	$\delta^{13}\text{C}$ (‰)	Lab-reported age (^{14}C yr BP at 1σ) [§]	Calibrated age (cal yr BP at 2σ) ^{**}	OxCal age (cal yr BP at 2σ) ^{##}
X	GX30259	02 MMZ	3.075	seeds	-24.8	4000 ± 30	4530-4410	
	GX30598	02 MMY	2.980	conifer needles	-26.9	4160 ± 30***	4830-4570	4830-4570
	GX30260	02 MMZ	3.085	seeds	-26.5	4190 ± 40***	4840-4570	
	<i>GX19887</i>	<i>93 C/T</i>	<i>3.600</i>	<i>twigs, bark fragments</i>	-28.7	<i>4398 ± 70</i>	5290-4830	
XI	GX30255	02 VB	4.285	tree stems/twigs	-27.3	4530 ± 40***	5320-5040	5450-5050
	GX30251	02 VB	4.285	deciduous leaves	-28.5	4630 ± 60***	5600-5050	
	<i>AA17179</i>	<i>94 BB</i>	<i>4.044</i>	<i>twig</i>	-24.1	4630 ± 65***	5600-5050	
XII	<i>AA19421</i>	<i>95 J</i>	<i>6.575</i>	<i>twig</i>	-25.5	5205 ± 65***	6180-5750	6180-5930
	GX30257	02 JB	6.410	spruce stems/needles, seeds	-26.6	5300 ± 40***	6200-5940	
	GX30258	02 JA	6.340	spruce needles, seeds	-29.1	5410 ± 40	6300-6000	

Note: data shown in italics from Kelsey et al. (2002).

*Radiocarbon age data grouped by buried soil number determined by stratigraphic correlation. Soil numbers increase with age.

[#]Lab abbreviations: AA, University of Arizona, NSF Accelerator Facility; GX, Geochron Laboratories, Cambridge, Massachusetts.

[†]Core number designates year sampled, and specific core identified by letter.

[§]Conventional ages reported by radiocarbon laboratory based on the Libby half life (5570) for ^{14}C . Bold ages are statistically indistinguishable at the 95% confidence level based on a chi-square test (Ward and Wilson, 1978).

**Calibrated age ranges before AD 1950 reported to the nearest decade, computed with OxCal (Bronk Ramsey, 2001) using the INTCAL98 radiocarbon calibration dataset of Stuiver et al. (1998) with a lab error multiplier of 1.0 and reported to 2σ .

Preferred calibrated age ranges based on stratigraphic analysis of radiocarbon ages and the means of statistically indistinguishable ages, where available, using OxCal (Bronk Ramsey, 2001).

^{††}Age range for soil II is estimated using the average sedimentation rate determined for soils VII to III, shown on Figure 5.

***Lab-reported ages used in OxCal analyses.

FIGURES

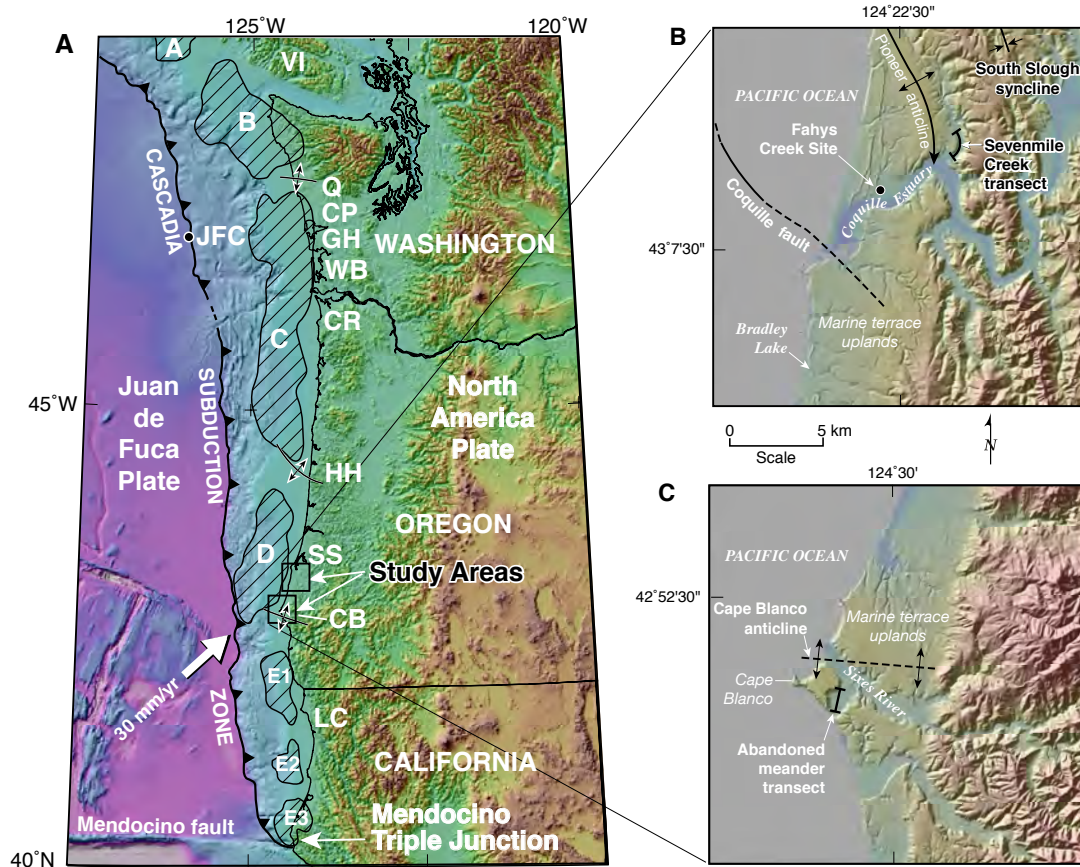


Figure 1. A: Map of the Juan de Fuca-North America plate boundary from Vancouver Island (VI) to northwestern California, showing regional tectonic setting of the study area. Coastal sites with stratigraphic evidence for Cascadia earthquakes include the Copalis River (CP), Grays Harbor (GH), Willapa Bay (WB), and the Columbia River (CR) in southwestern Washington, and South Slough (SS), the Coquille River estuary (Figure 1B), and the Sixes River (Figure 1C) in southwestern Oregon. Strata at Lagoon Creek (LC) in northern California record Cascadia tsunamis. Turbidites triggered by Cascadia earthquakes and deposited in the Juan de Fuca Canyon (JFC) and other submarine channels on the continental slope record 18 events in the Holocene (Goldfinger et al., 2003). Offshore gravity lows (A-E) that coincide with Cascadia forearc basins are interpreted to correlate with regions of long-term coseismic slip on the subduction zone (Wells et al., 2003). Active transverse upper-plate structures at Quinault (Q), Heceta Head (HH), and Cape Blanco (CB) accommodate margin parallel shortening and define candidate Cascadia segment boundaries analogous to L-shaped structural highs that separate structural segments of the Nankai Trough in southwestern Japan (Sugiyama, 1994). White arrow indicates Juan de Fuca plate motion relative to North America (Miller et al., 2001). B: Sevenmile Creek transect (Figure 2A) and Fahys Creek core site located along the Coquille River estuary where upper-plate structures, including the Coquille fault (McInnelly and Kelsey, 1990), deform late Pleistocene marine terraces. Bradley Lake records tsunamis and seismic shaking generated on the Cascadia margin over the last 7,000 years (Kelsey et al., in press). C: Sixes River transect (Figure 2B) located in abandoned meander near Cape Blanco. The Cape Blanco anticline deforms Pleistocene marine terraces and Holocene marsh strata (Kelsey, 1990; Kelsey et al., 2002).

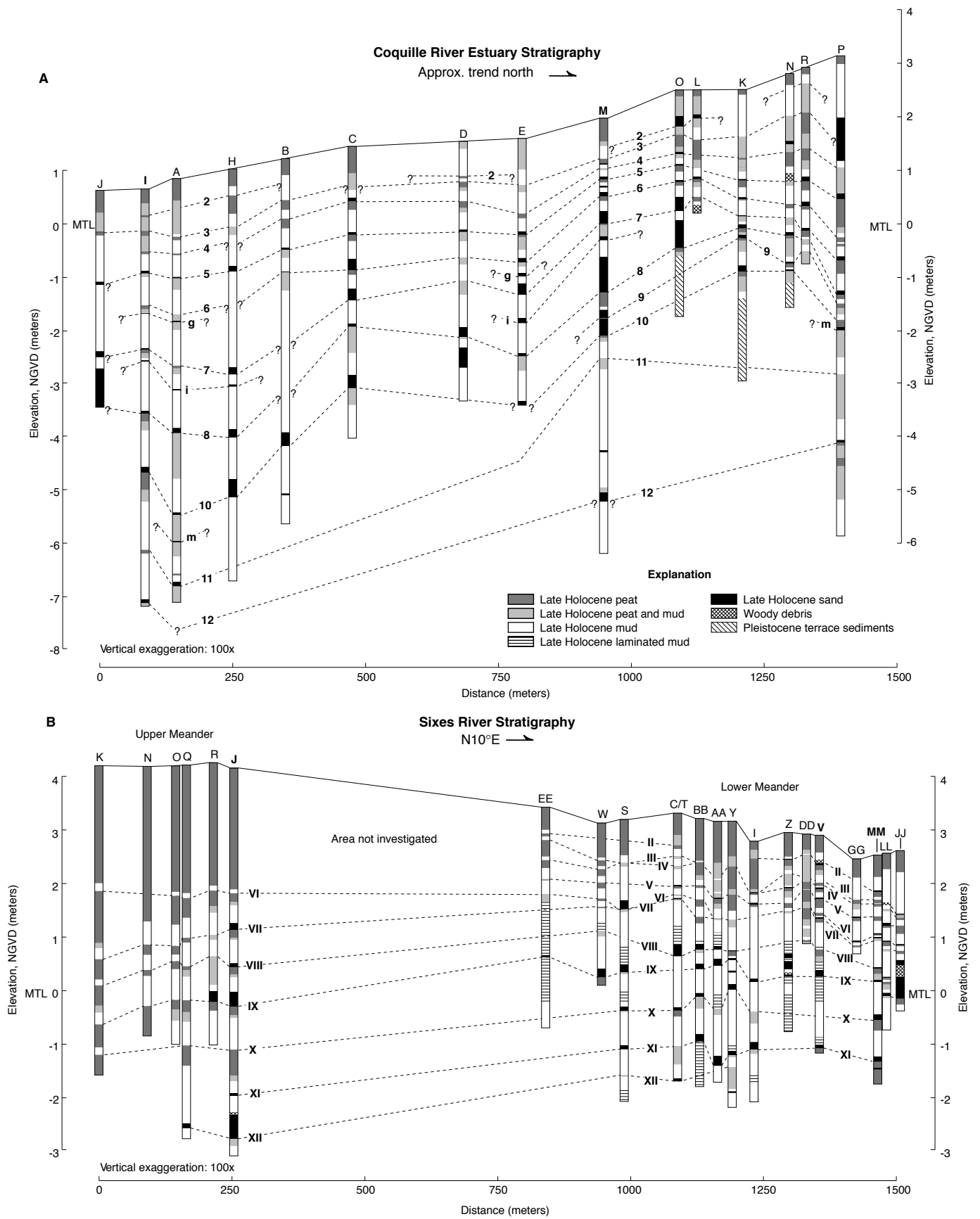


Figure 2. Stratigraphy from the Coquille River estuary at Sevenmile Creek (A) and the lower Sixes River Valley near Cape Blanco (B). Arabic and Roman numerals designate former marsh surfaces buried by sand and mud at the Coquille and Sixes sites, respectively. Dashed lines connect correlative buried soils. Core elevations based on surveyed profiles accurate to ±0.05 m at Coquille and ±0.01 m at Sixes. Bold letters identify vibracores shown in detail on Figure 3. Fahys Creek core O not shown here. MHHW—mean higher high water; MTL—mean tide level; MLLW—mean lower low water; NGVD—National Geodetic Vertical Datum, 1929.

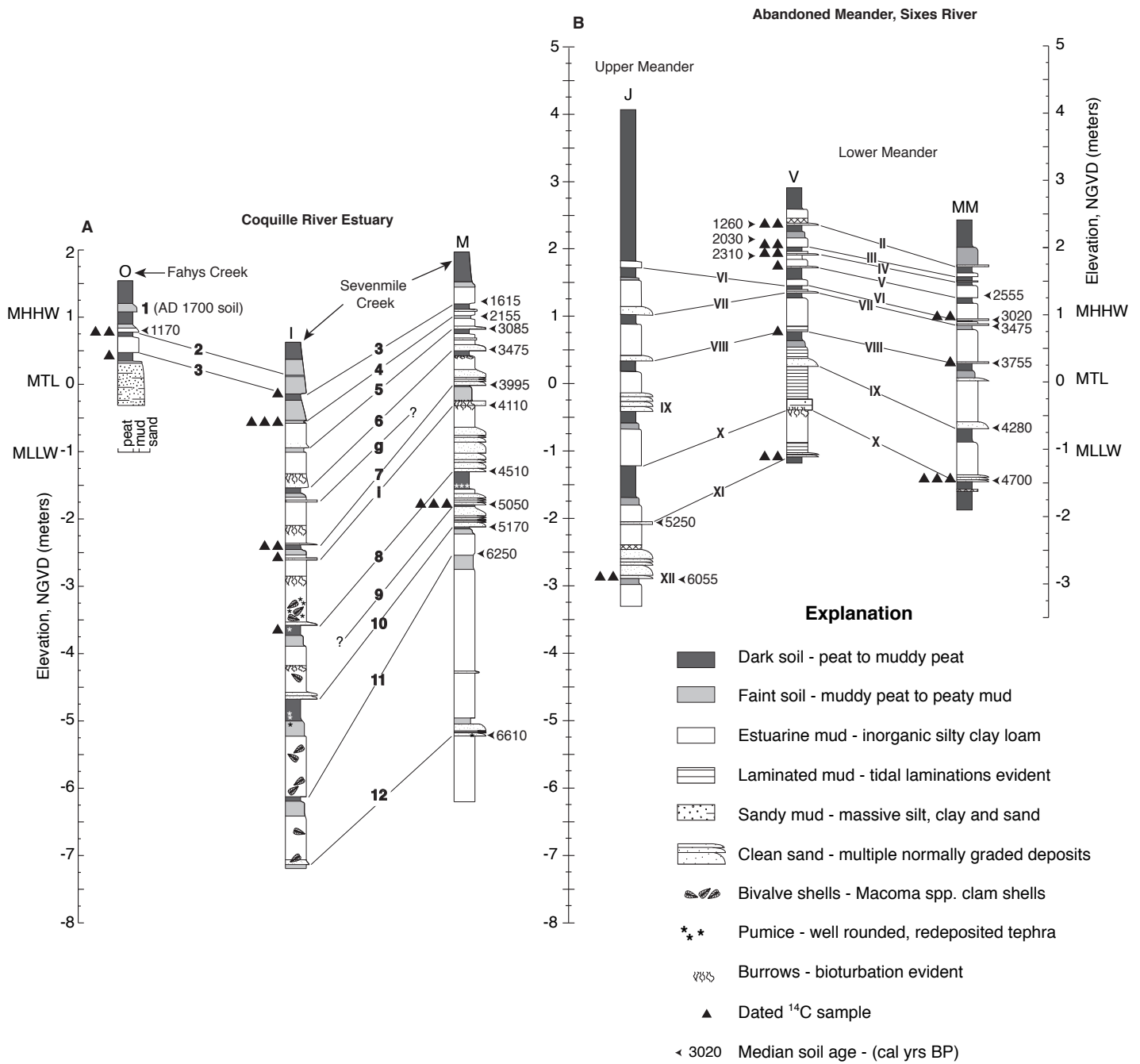


Figure 3. Detailed lithostratigraphy of vibracores collected at the Coquille River estuary and the lower Sixes River Valley. A: Core O from Fahys Creek and cores I and M from Sevenmile Creek together preserve stratigraphic evidence of 12 episodes of sudden marsh submergence in the last 6,300 years (soils 1 through 12). B: Cores J, V and MM from the abandoned meander in the lower Sixes River Valley record the sudden submergence of 11 marsh soils in the last 5,500 years. MHHW—mean higher high water; MTL—mean tide level; MLLW—mean lower low water; NGVD—National Geodetic Vertical Datum, 1929.

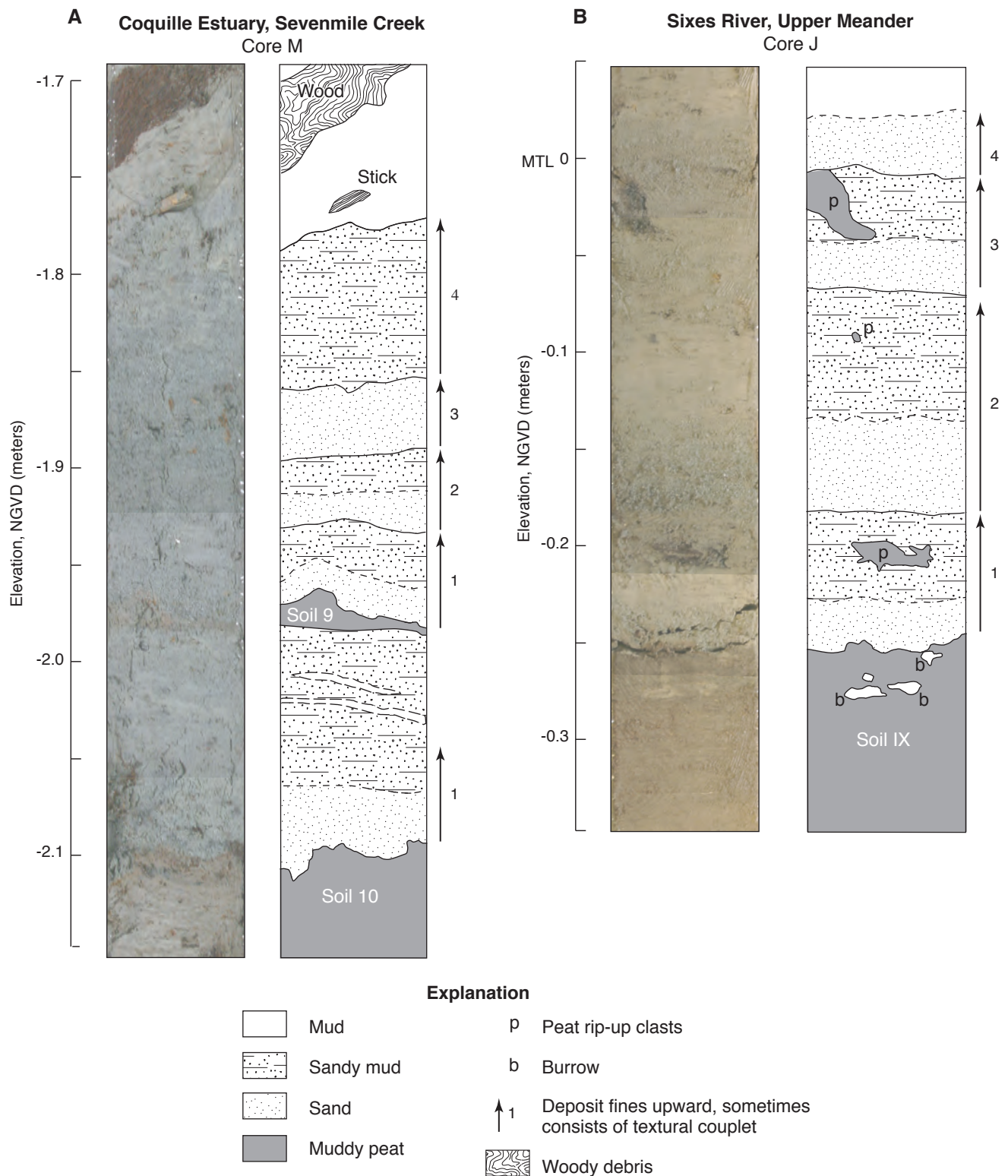


Figure 4. Core photographs and interpretive sketches of multiple fining-upward beds within sand deposits that bury tidal marsh soils. A: Sand deposits overlying soils 10 and 9 in core M from the Coquille estuary at Sevenmile Creek. Four fining-upward sand beds overlie soil 9; whereas, only one fining-upward sand bed overlies soil 10. Soil 9 and overlying sand beds were observed in few cores and lack the widespread distribution of other soils buried by sand interpreted to record coseismic subsidence and tsunami inundation B: Four fining-upward beds overlying buried soil IX in core J at the Sixes River site. Irregular upper soil contact and mud clasts within sand indicate erosion during sand deposition. Burrows indicate bioturbation of upper part of soil IX. MTL—mean tide level; NGVD—National Geodetic Vertical Datum, 1929.

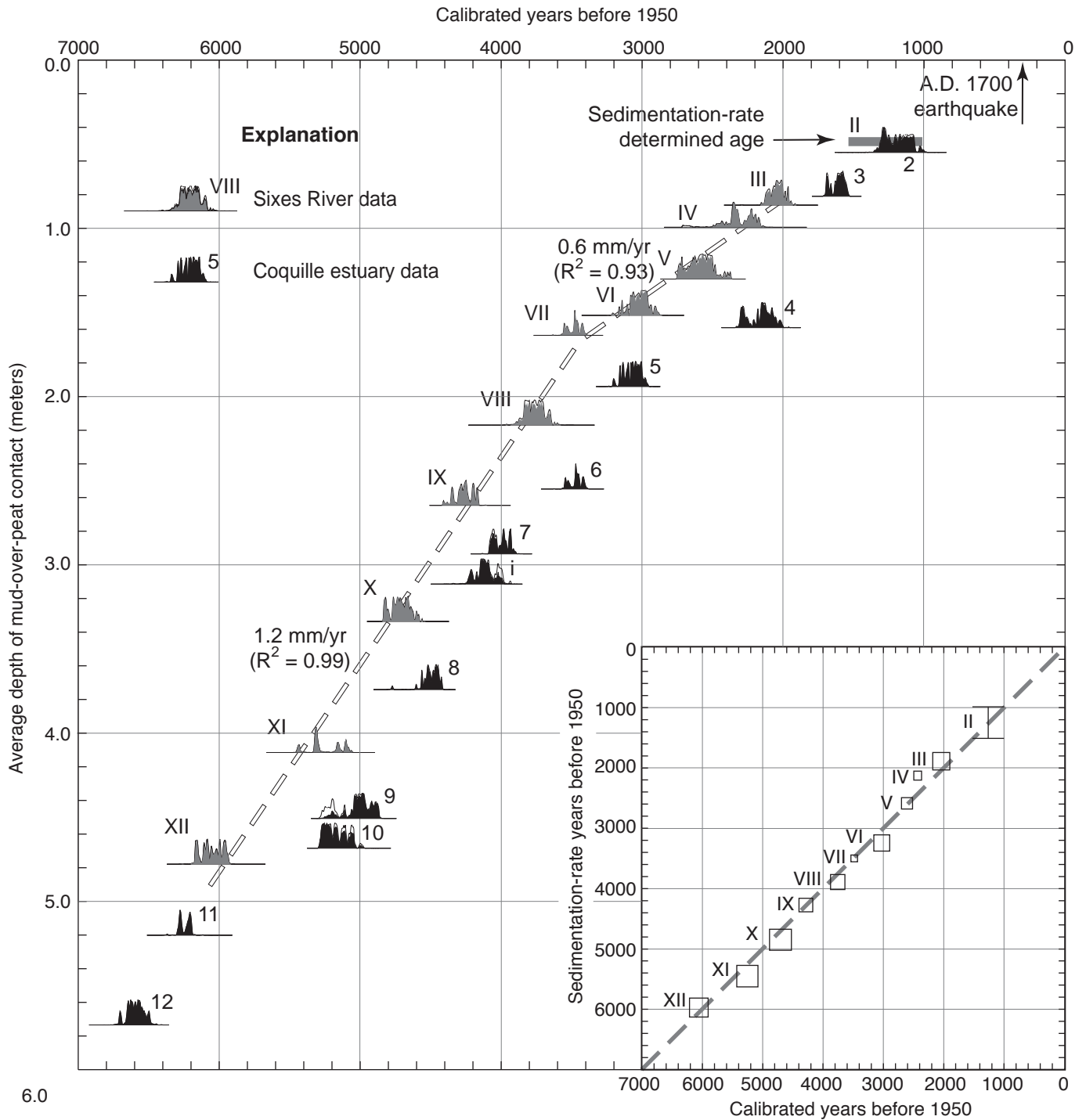


Figure 5. Calibrated radiocarbon-age distributions (years before AD 1950) calculated with the program OxCal (Bronk Ramsey, 2001) for detrital macrofossils selected from buried marsh soils and overlying mud and sand deposits in the lower Sixes River valley and Coquille River estuary. Final age distributions for Sixes River soils (grey) and Coquille estuary soils (black) were statistically restricted where initial distributions (white) overlapped through sequence analysis with the OxCal program. Roman numerals indicate soils dated at the Sixes River; Arabic numbers indicate soils dated at the Coquille estuary. Dashed lines show a variation in linear regression lines for average sedimentation rates prior to and post 3,500 yr BP based on calibrated-age ranges for soils X to VIII and VII to III, respectively, at the Sixes River. The age for soil II is estimated using the average sedimentation rate determined for soils VII to III. Inset diagram compares calibrated radiocarbon-age estimates to age estimates derived from average sedimentation rates derived from Sixes River data.

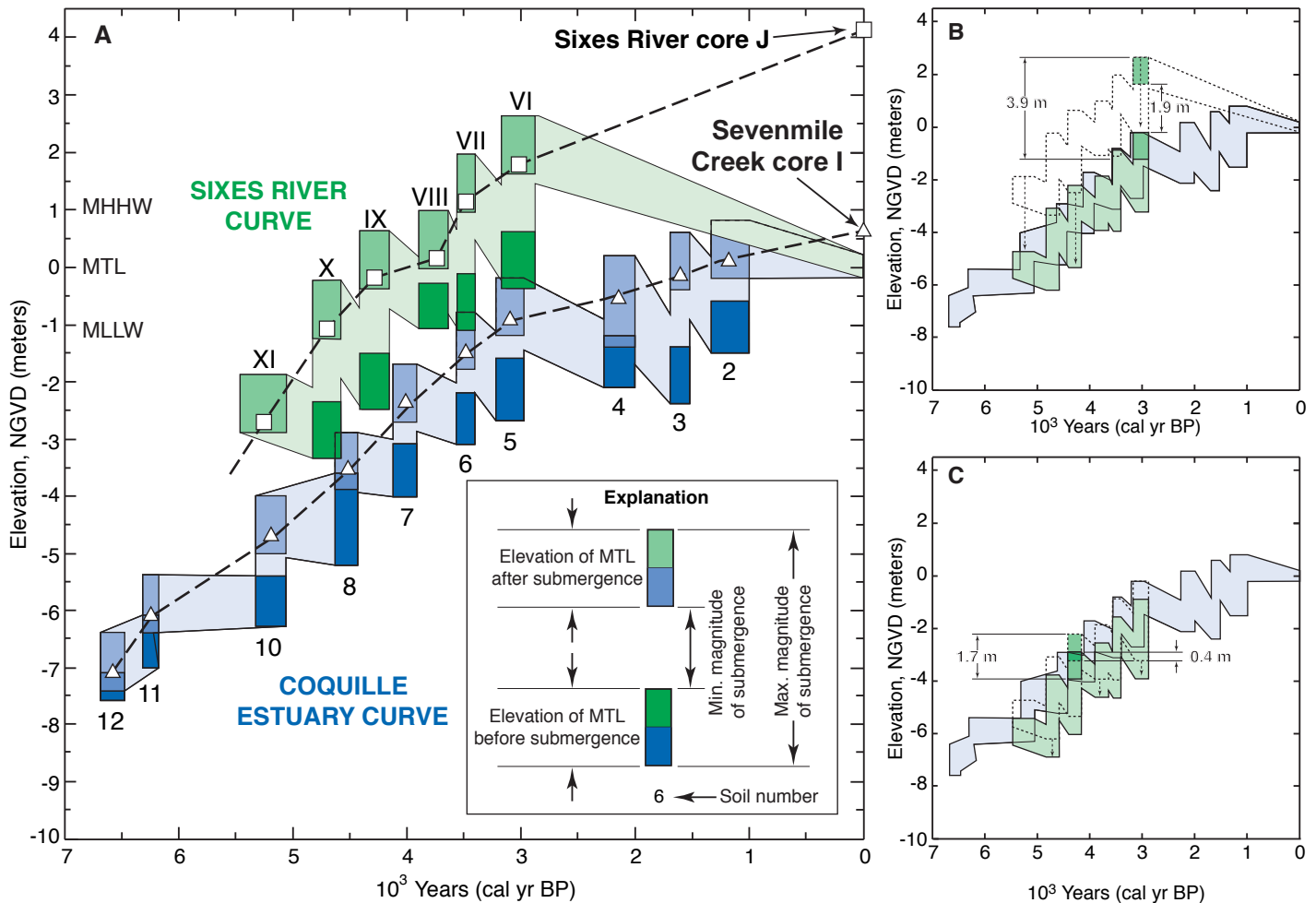


Figure 6. A: Relative sea-level curves for Coquille River estuary (blue) and the lower Sixes River valley (green). Widths of rectangles delineate time of soil burial based on radiocarbon age estimates (Table 1). Heights of rectangles estimate elevations of MTL based on fossil diatom assemblages from soil (darkest shade) and overlying mud (intermediate shade) reported in prior studies (Kelsey et al., 2002; Witter et al., 2003). Envelopes that encompass rectangles track changes in elevation of MTL through time and incorporate uncertainties related to radiocarbon age estimates and the paleo-elevation of MTL. Relative sea-level curve depicts episodes of instantaneous relative sea-level rise followed by periods of more gradual sea-level change. Triangles mark elevations of the upper contacts of buried soils in core I; squares mark elevations of the upper contacts of soils in core J. Dashed line reflects sediment aggradation rate. MHHW—mean higher high water; MLLW—mean lower low water; NGVD—National Geodetic Vertical Datum. B: Reconstruction of a single sea-level curve to estimate the variation in upper-plate vertical deformation between Cape Blanco and the Coquille River estuary in the last 3,000 years. A vertical shift of 1.9 to 3.9 m is necessary to restore the Sixes River curve to the same elevation as the Coquille curve. C: Reconstructing the Sixes River curve to match the elevation of the Coquille curve at about 4,300 years ago requires a shift of 0.4 to 1.7 m. This shift estimates the variation in upper-plate deformation at the two sites between 4,300 to 3,000 years ago.

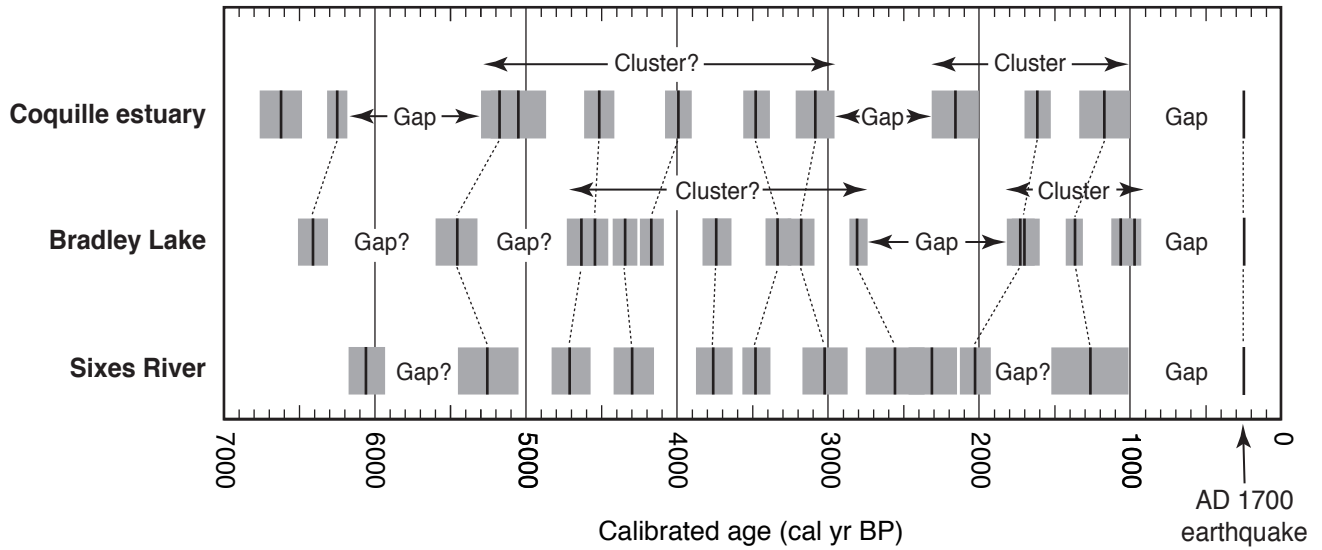


Figure 7. Frequency of earthquakes and tsunamis above the Cascadia subduction zone in southwestern Oregon. Age ranges (2σ) for Coquille estuary and Sixes River earthquake records from Tables 1 and 2, respectively. Age ranges (2σ) for Bradley Lake tsunami record from Kelsey et al. (in press). Dashed lines indicate possible correlations among earthquakes and tsunamis in southern coastal Oregon.

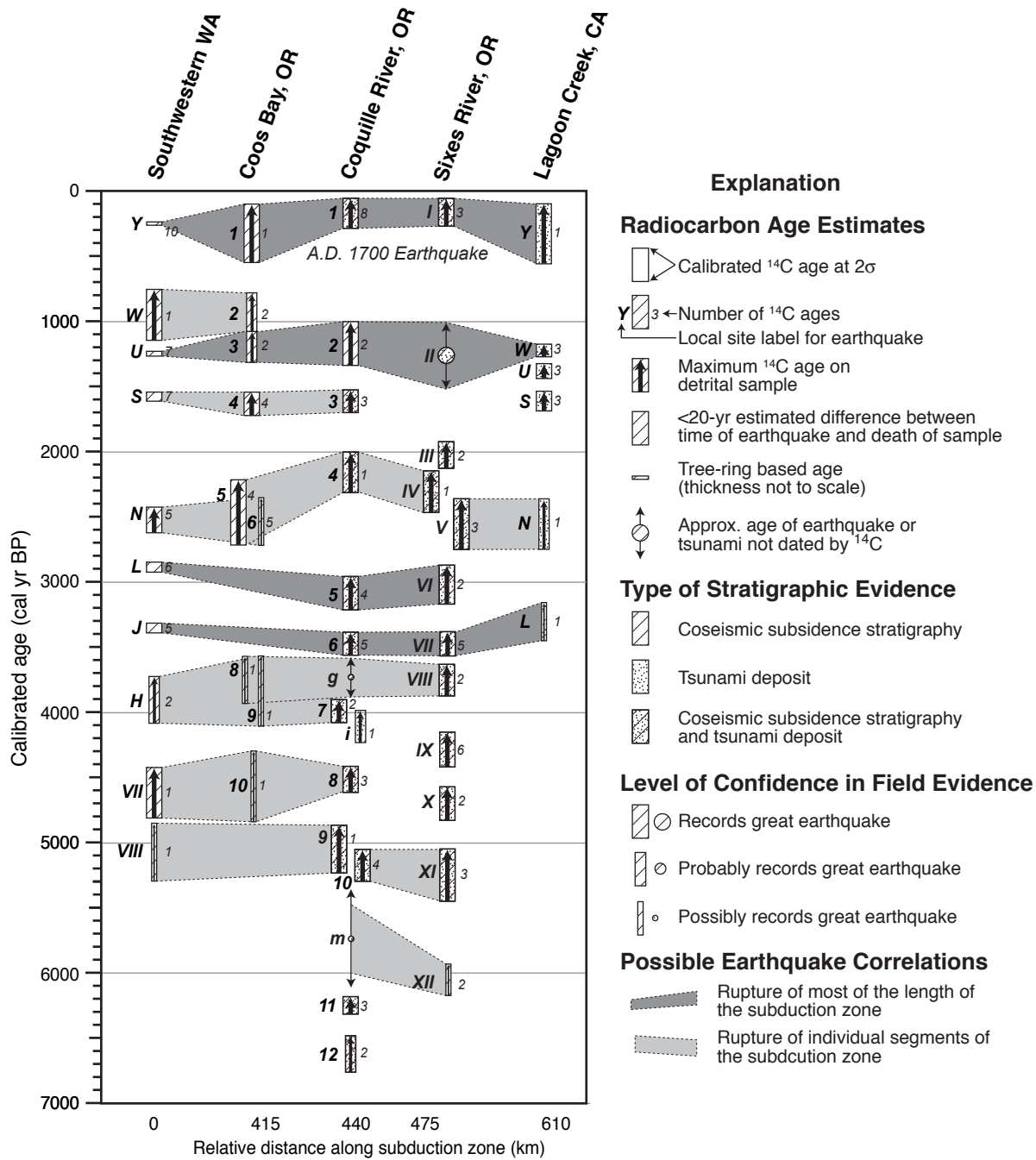


Figure 8. Comparison of calibrated age ranges for Cascadia subduction zone earthquakes and tsunamis at the Coquille River estuary and the lower Sixes River valley, to data from Coos Bay, Oregon (Nelson et al., 1996, 1998; Nelson, unpub. data) and southwestern Washington (Atwater and Hemphill-Haley, 1997; Atwater, unpub. data). Arabic and Roman numerals designate buried soils at the Coquille River estuary and Sixes River sites as shown in Figures 2 and 3. Darkest shaded zones indicate possible correlations among earthquakes that may have ruptured most of the length of the subduction zone. Lighter zones show possible correlations for shorter ruptures. Individual age ranges that do not overlap with age ranges at adjacent sites and different numbers of events over similar time periods at separate sites imply that not all Cascadia subduction zone earthquakes ruptured the entire plate boundary from southwestern Washington to southern Oregon.